Published in final edited form as:

Brain Res. 2004 December 24; 1030(1): 28–48. doi:10.1016/j.brainres.2004.09.034.

Distribution of methionine and leucine enkephalin neurons within the social behavior circuitry of the male Syrian hamster brain☆

Avril Genene Holt[a,*] and **Sarah Winans Newman**[b]

[a]Kresge Hearing Research Institute, University of Michigan, 1301 East Ann Street, Ann Arbor, MI 48109, USA

[b]Department of Cell and Developmental Biology, University of Michigan, Ann Arbor, MI 48109, USA

Abstract

Enkephalin plays a role in the social behaviors of many species, but no corresponding role for this peptide has been investigated in the male Syrian hamster, a species in which brain nuclei controlling social behaviors have been identified. Previous studies have shown the distribution of dynorphin and beta-endorphin throughout social behavior circuits within the male hamster brain. To date, the only studies of enkephalin in the hamster brain address the distribution of this peptide in the olfactory bulb and hippocampus. The present study provides a complete map of enkephalinergic neurons within the forebrain and midbrain of the male Syrian hamster and addresses the question of whether enkephalin immunoreactive (Enk-ir) cells are found within brain regions relevant to male hamster social behaviors. Following immunocytochemistry for either methionine enkephalin (met-enkephalin) or leucine enkephalin (leu-enkephalin), we observed enkephalin localization consistent with data that have previously been reported in the rat, with notable exceptions including lateral septum, ventromedial nucleus of the hypothalamus and cingulate gyrus. Additionally, met- and leu-enkephalin localization patterns largely overlap. Consistent with the post-translational processing of preproenkephalin, met-enkephalin was more abundant than leu-enkephalin both within individual cells (darker staining), and within given brain nuclei (more met-enkephalin immunoreactive cells). Two exceptions were the posterointermediate bed nucleus of the stria terminalis, containing more neurons heavily labeled for leu-enkephalin, and the main olfactory bulb, where only met-enkephalin was observed. Of most interest for this study was the observation of Enk-ir cells and terminals in areas implicated in both sexual and agonistic behaviors in this species.

Keywords

Mating; Agonistic behavior; Sexual behavior; Opioid; Neuropeptide

☆Predoctoral Fellowship awarded to AGH from NIH-1F31GM013553. Awarded to SWN from NIH-NS20629.

*Corresponding author. Tel.: +1 734 763 4385; fax: +1 734 764 0014. avrilhol@umich.edu (A.G. Holt).

1. Introduction

The well-delineated limbic circuits that mediate sexual behavior and aggression in the male Syrian hamster make this animal an excellent model for the study of social behaviors. Specifically, neuroanatomical connections [15,19,22,25,29,40,60,71] and sex hormone receptor distribution, [13,16,58,103] as well as behavioral correlates of lesions [8,17,23,54–56,67,74,79,102] and of increased c-fos expression [22,26,38,47–50,89,104] have been determined for many areas within these circuits. Much less is known about the chemical neuroanatomy of social behavior pathways in the hamster.

The distribution and pharmacology of neurotransmitters and neurotransmitter receptors that influence social behaviors has been investigated extensively in the rat (reviewed in Meisel and Sachs [63]). These same neurochemicals may also regulate social behaviors in the golden hamster. However, documented species differences in the distribution of several transmitters preclude the assumption that the chemical neuroanatomy of circuits in the hamster brain is the same as that of the rat. For example, substance P is abundant in the nuclei of the mating behavior pathway in both rat [11,31] and hamster [71,72], whereas CCK, which is heavily distributed in these areas in rat, appears to be absent in hamster [64,85]. In contrast, both dopamine [5] and dynorphin [70] have been localized in areas of the hamster's sexual behavior pathway where neither is observed in the rat.

The social status and behavioral experience of an individual animal have been shown to have significant influence over the production and stored levels of enkephalin in the brain. In a variety of rodents, the concentration of enkephalin found in the brain can vary with the dominance status of the animal [24,51,78,80]. Further, in the male rat, Agmo et al. [3] have demonstrated that enkephalin levels influence mating behavior. If enkephalin also influences social behaviors in the hamster, then immunoreactivity for enkephalin peptides should be detected within brain regions, which regulate these behaviors. Thus, we have investigated the distribution, behaviorally induced activation, and sex steroid regulation of the endogenous opioid, enkephalin, within the social behavior circuitry of the hamster brain.

As the first in a series of reports, the results reported here indicate that in the hamster, methionine (met-) and leucine (leu-) enkephalin are localized within pathways that regulate mating and aggressive behavior.

2. Materials and methods

2.1. Animals

The brains of eight male Syrian hamsters weighing between 110 and 200 g were studied. The animals were group housed in a long day photoperiod (10 h dark and 14 h light) and had access to food and water at all times.

2.2. Tissue preparation for Immunocytochemistry

Prior to perfusion six males received an intracerebral ventricular (i.c.v.) injection of 200 μg colchicine, to inhibit axonal transport. This dose had been determined to be optimal in preliminary experiments. Colchicine dissolved in 2.5 μl of 0.9% saline was stereotaxically

delivered into the left lateral ventricle in animals anesthetized with sodium pentobarbital (10 mg/100 g body weight). Stereotaxic coordinates were +1.5 AP, +1.5 ML, and −3.3 DV (from bregma) with bregma and lambda in the same horizontal plane. After 48 h each animal was deeply anesthetized with sodium pentobarbital (15 mg/100 g) and perfused through the ascending aorta with 150 ml of 0.1 M sodium phosphate-buffered saline (PBS) followed by 250 ml of 4% paraformaldehyde in PBS with 0.1% sodium nitrite for vasodilatation. The brains were removed from the skull and post-fixed for 1 h in the same fixative, then immersed overnight at 4 °C in 20% sucrose in PBS for cryoprotection. Using a freezing microtome, each brain was cut coronally into 40-μm sections that were collected serially into 12 vials containing PBS with 0.01% sodium azide. Two additional animals were perfused without prior injection of colchicine, to optimize staining of enkephalinergic fibers and terminals; their brains were processed as described above.

2.3. Met- and leu-enkephalin immunocytochemistry

Met- and leu-enkephalin polyclonal antibodies produced in rabbit (ImmunoStar, Hudson, WI [formerly Incstar]) were used to determine the enkephalin distribution reported here. Initially four different concentrations of antibody (1:250, 1:500, 1:1000, and 1:5000) were tested to determine the optimal concentration for enkephalin immunoreactivity. Free floating sections (every 4th section through the forebrain and midbrain) were incubated in one of the primary antibodies, with normal donkey serum (1:200; Jackson Laboratories) and 0.3% Triton X-100 in potassium phosphate-buffered saline (KPBS) for 48 h at 4 °C on a rotator. All subsequent incubations and rinses (3 × 5 min in KPBS) were done at room temperature. The tissues were then rinsed and incubated for 1 h on a rotator in biotinylated donkey anti-rabbit secondary antibody (1:100, Jackson Laboratories) and normal donkey serum (1:200, Jackson Laboratories) in 0.3% Triton X-100 in KPBS. After rinsing, they were incubated with avidin–biotin complex (Vectastain Elite kit, Vector Labs) in KPBS for 1 h on a rotator before the avidin–biotin/HRP complex was visualized using nickel chloride enhanced diaminobenzidine (one 10 mg diaminobenzidine tablet from Sigma dissolved in 80 ml KPBS and 200 μl H_2O_2 with 250 μl NiCl) developed over a 6-min period on a shaker. Adjacent sections were stained with cresyl violet to assist in cytoarchitectonic localization of enkephalin. The sections were mounted from KPBS onto gelatin-coated slides, air-dried, dehydrated, and coverslipped using Permount.

2.4. Control procedures

In the descriptions of control procedures below, a “vial” contains serially spaced 40-μm sections representing every 12th section through the brain.

2.4.1. Preabsorption of antibody with peptide—For each of the primary antibodies studied, one vial of sections from each brain was preabsorbed with either 10 or 75 μM met-enkephalin (Bachem) or a 10 or 75 μM concentration of leu-enkephalin (Bachem) for 1 h at room temperature, after which the standard immunohistochemical procedure was followed. Tissues prepared in these four control conditions were compared to tissues processed simultaneously but without peptides in the preincubation medium.

2.4.2. Omission of the primary and secondary antibodies—In two vials of sections from each brain that had been injected i.c.v. with 200 μg of colchicine, the primary antibody (either met- or leu-enkephalin) was replaced with an equal volume of KPBS. Two additional vials of sections from each brain were processed with the primary antisera (one with met- and one with leu-enkephalin) but with KPBS replacing the secondary antiserum, biotinylated donkey antirabbit. These procedures allowed us to determine that the immunolabeling observed was not a result of nonspecific labeling. These control tissues were processed concurrently with sections prepared for met- and leu-enkephalin immunohistochemistry.

2.5. Histological and data analysis

The distribution of enkephalin immunoreactive cells, fibers, and puncta from all animals was plotted onto camera lucida drawings of adjacent cresyl violet stained brain sections. Immunoreactive fibers were differentiated from puncta by the clearly visible axon linking varicosities (Fig. 1A). The terminal fields (puncta and en passant swellings) appeared as clusters of immunostained dots forming a cloud (Fig. 1B). Cell bodies were counted only if the pale unstained nucleus was discerned within the immunostained cytoplasm.

3. Results

3.1. Immunolabeling controls

The optimal dilution used for immunolabeling with both antibodies was 1:1000. In general, the brain distribution of met- and leu-enkephalin immunoreactivity overlapped (Table 1), but the met-enkephalin immunoreactivity was greater than leu-enkephalin immunoreactivity in quantity (number of neuronal elements) and quality (intensity) (Fig. 2A,B). This was observed throughout the forebrain, with two exceptions: in the olfactory bulbs only met-enkephalin immunoreactivity was found, and in the posterointermediate subdivision of the bed nucleus of the stria terminalis (BNSTpi) the leu-enkephalin immunoreactivity was reliably greater in quantity as well as quality than the met-enkephalin immunoreactivity.

Omission of the primary or secondary antibody from the incubation solutions resulted in no staining (Fig. 3A and B). Preabsorption of the met-enkephalin antibody with 10 μM met-enkephalin resulted in no staining (Fig. 3C) while the preabsorption of the met-enkephalin antibody with 75 μM leu-enkephalin resulted in normal met-enkephalin staining (Fig. 3D). Likewise, the preabsorption of the leu-enkephalin antibody with 10 μM leu-enkephalin resulted in no staining (Fig. 3E). Preabsorption of the leu-enkephalin antibody with 75 μM met-enkephalin resulted in a slight apparent decrease in leu-enkephalin immunoreactivity throughout the brain (Fig. 3F). In order to assess the effect of this decreased labeling, leu-enkephalin immunoreactive cells were counted in the medial septum and the periaqueductal gray. The counts revealed no difference in the mean number of leu-enkephalin immunoreactive cells between preabsorbed and non-preabsorbed sections from these two regions in the same brain (Table 2; n=6 brains analyzed for each region; PAG p=0.645; septum p=0.191).

3.2. Colchicine effects

Visualization of terminals and fibers throughout the brain was possible without the use of colchicine (compare Fig. 4A and B), but to visualize the enkephalinergic cell bodies our preliminary experiments had demonstrated that a dose of at least 50 μg of colchicine was necessary (compare Fig. 4C and D). Only in the hippocampus were cell bodies observed without colchicine (compare Fig. 4E and F). As noted previously, optimal immunolabeling was achieved with a colchicine dose of 200 μg.

3.3. Neuroanatomical distribution of enkephalin immunoreactivity

Figs. 5A–F and 6A–F are examples of met-enkephalin immunoreactive cells, fibers, and puncta to illustrate the appearance of immunolabeling in selected areas of the telencephalon, diencephalon, and midbrain. Figs. 7–14 are tracings of selected coronal sections of the hamster brain illustrating the distribution of met-enkephalin immunoreactive cells, fibers and terminals throughout the forebrain and midbrain. The identification of, and terminology for, anatomical areas in the hamster brain is consistent with Morin and Wood [66].

3.4. Localization of enkephalin immunoreactive elements

3.4.1. Cortex—Many areas of the isocortex caudal to the frontal poles contain met- and leu-enkephalin immunoreactive cell bodies. These cells are seen predominantly in layer VI (Figs. 8–14). The cells are large, pyramidal-shaped and darkly stained with long processes extending towards the more superficial layers of the cortices (Fig. 5A). The frontal pole (Fig. 7A) does not contain labeled cells.

In the piriform cortex (Pir), both cells and fibers containing met- and leu-enkephalin are observed in layer II, but their distribution across the rostro-caudal extent of this cortex is not uniform. In the most rostral region (Fig. 7) the piriform cortex is devoid of enkephalin immunoreactivity, whereas in the mid-portion (Figs. 8 and 9) both immunoreactive cells and fibers are found. In the caudal piriform cortex (Figs. 10 and 11) immunoreactive staining was highly variable, with only cells or only fibers at some levels and no staining at all at other levels.

3.4.2. Striatum and pallidum—In the striatum and the pallidum (Fig. 5B), met- and leu-enkephalin immunoreactive fibers and terminals predominate.

3.4.2.1. Ventral striatum and ventral pallidum: The core of the nucleus accumbens (AcbC) contains a patchy fiber network with a few cells scattered throughout the nucleus (Figs. 7 and 8) while the substriatal gray or fundus striati (FStr; Fig. 9) contains no cells or fibers. In the olfactory tubercle (Tu), a meshwork of darkly stained fibers and/or terminals is found in layer II and is especially prominent within the islands of Calleja (ICj) and the insula Calleja magna. Immunoreactive cells are sparse and are predominantly found in the rostral olfactory tubercle (Fig. 7). The caudal part of the ventral pallidum (VP; Fig. 9B) contains a dense plexus of darkly stained fibers and terminals.

3.4.2.2. Caudate/putamen and globus pallidus: The caudate/putamen (CP) has enkephalin positive fibers and cells throughout its rostro-caudal extent (Figs. 7–11). Rostrally, labeled

cells are more apparent laterally; however the plexus of heavily labeled enkephalin fibers in the medial CP hampers our ability to clearly discern labeled cells in this region. The darkly labeled, enkephalin fiber plexus of the globus pallidus (GP) is present throughout the nucleus (Figs. 9–11). As in the caudate/putamen region, in the globus pallidus the extensive labeling of the enkephalin fibers obscures labeled cells (Fig. 4A,B).

3.4.3. Septum—Met- and leu-enkephalin immunoreactivity is found predominantly in two septal regions. The ventral lateral septum (LSv) is covered with a dense fiber plexus including puncta (Figs. 5C and 9), while the medial septum (MS) contains primarily met- and leu-enkephalin immunoreactive cell bodies with very few fibers (Figs. 5D and 9). Rostrally, the intermediate lateral septum (LSi) contains a patch of enkephalinergic puncta (Fig. 8B) while at more caudal levels no enkephalin staining is present in this region of the septum.

3.5. Horizontal Limb of the nucleus of the diagonal band of Broca (HLNDB)

A dense, darkly stained network of fibers extends throughout the horizontal nucleus of the diagonal band of Broca (Figs. 8–10). A few, scattered enkephalinergic cells are found throughout this nucleus, with the exception of a more numerous population of met- and leu-enkephalin cells in the mid-caudal HLNDB, at the level of the rostral medial preoptic nucleus (Fig. 9B).

3.5.1. Bed nucleus of the stria terminalis (BNST)—The terminology used here is from Gomez and Newman [29], Kollack–Walker and Newman [48], and, with the exception of the designation of the anterolateral bed nucleus of the stria terminalis, is consistent with the terminology of Morin and Wood [66]. At the most rostral extent of the bed nucleus of the stria terminalis (BNST) where the fibers of the anterior limb of the anterior commissure pass medially beneath the lateral ventricles, the anterolateral (al) and anteromedial (am) BNST, dorsal to the anterior commissure, contain met- and leu-enkephalin cell bodies (Figs. 5E and 9). The anteroventral (av) BNST at this level contains only enkephalinergic fibers and no cells.

The anterodorsal portion of the posteromedial (pm) BNST (Fig. 10A) and the posterointermediate (pi) BNST at the level of the body of the anterior commissure contain both met- and leu-enkephalin immunoreactive cells, some fiber staining and no detectable puncta staining. However, in the posterointermediate BNST, both the number of leu-enkephalin immunoreactive cells and the intensity of labeling are greater when compared to met-enkephalin immunoreactivity. This is the only region of the brain in which leu-enkephalin immunoreactivity predominates. The posterolateral (pl) BNST contains only a very few enkephalinergic cells and light fiber staining (Fig. 10A).

3.5.2. Preoptic area—The terminology used here is from Maragos et al. [60] as well as Morin and Wood [66]. Numerous darkly stained enkephalinergic cells and few fibers are distributed throughout the rostral-caudal extent of the median preoptic nucleus (MPN; Figs. 5F, 9, and 10), the magnocellular MPN (MPNmag; Fig. 10), and the lateral preoptic area (LPOA; Fig. 10). In general, many more cells, fibers, and puncta are found in the rostral

two-thirds of the medial preoptic area (MPOA) than in the caudal one-third, which contains few cells and no fibers or terminals (Figs. 10 and 11). The enkephalin immunoreactive cells throughout the preoptic area exhibit a large nuclear to cytoplasmic ratio when viewed in the coronal plane of section.

3.5.3. Anterior hypothalamus (AH)—The anterior hypothalamus contains met- and leuenkephalin immunoreactive cells distributed throughout, while fibers and terminals in this area are sparse (Figs. 6A, 11, and 12).

3.5.4. Paraventricular nucleus of the hypothalamus (PVN)—The paraventricular nucleus of the hypothalamus is cytoarchitectonically divided into several subnuclei by Morin and Blanchard [65]. However, here we distinguish only the medial and lateral portions of this nucleus. In general, cells are predominantly located medially with fibers and some puncta laterally (Figs. 6C, 11, and 12A). The zona incerta (ZI) contains both cells and fibers with more fibers in the caudal portion of the nucleus (Fig. 11).

3.6. Ventromedial nucleus of the hypothalamus (VMH)

Although there are a few met- and leu-enkephalin immunoreactive cells scattered throughout the VMH, the majority of enkephalinergic cells are clustered in the lateral VMH (Figs. 6B, 12B, and 13A), whereas the fibers and puncta which are scattered throughout the nucleus form a cluster medially.

3.6.1. Amygdala—The terminology for the nuclei of the amygdala utilized in this paper is based on Gomez and Newman [28,29] and consistent with Morin and Wood [66]. The massa intercalata (MI) contains only a few intensely labeled cells and no fibers or terminals (Fig. 12A). The central nucleus (Ce) is filled with dense fiber staining with a few moderately stained cells dispersed throughout (Figs. 6E, 12B, and 13). Although there are clear cytoarchitectonic and connectional differences between the medial and lateral portions of this nucleus, our results do not reveal any differences based upon enkephalin staining. The anterodorsal (MeAD), anteroventral (MeAV), and posterodorsal (MePD) subdivisions of the medial nucleus primarily contain fiber and terminal staining, with an occasional cell located in the molecular layer adjacent to the optic tract (Figs. 6D, 11, and 12). The posteroventral subdivision of the medial nucleus (MePV) contains no enkephalin immunolabeled elements. The anterior cortical nucleus contains very little fiber and terminal staining, but contains a small number of medium-sized lightly stained cells (Figs. 11B and 12A). The anterior basolateral nucleus (BLa) contains a moderate number of cells and light fiber and terminal staining (Figs. 11 and 12). No enkephalin immunoreactivity is present in the posterolateral cortical, posteromedial cortical, or basomedial amygdaloid nuclei.

3.6.2. Hippocampal formation—The hippocampal formation contains intense immunoreactivity in the hilus of the dentate gyrus and in the mossy fiber system. Immunoreactive processes are seen in the dentate molecular layer and scattered throughout the CA1 and CA3 fields. An additional plexus of enkephalinergic fibers is found along the hippocampal fissure. Cells immunoreactive for enkephaln are located in and just superficial to the dentate granule cell layer (Figs. 11–14). These cells are visible even without

colchicine treatment (Fig. 4E–F). There are no enkephalin immunoreactive elements in the CA1 region of the hippocampus with the exception of fibers in its most caudal region. Enkephalin immunoreactive cells are present throughout the CA3 region except in the ventral half of the most posterior portion of the CA3.

3.6.3. Olfactory bulb—Immunoreactivity is only observed in the olfactory bulb with a concentration of primary antibody at 1:250 using the met-enkephalin antibody. No leu-enkephalin immunoreactive elements are found in this brain area at any of the concentrations of antibody we used (1:250, 1:500, 1:1000, and 1:5000). In the glomerular layer, met-enkephalin immunoreactivity is seen in the somata and dendrites of external tufted cells. Met-enkephalin immunoreactivity is also observed in the internal granule cells.

3.6.4. Periaqueductal gray (PAG)—Met- and leu-enkephalin immunoreactivity is found in the rostral PAG at the level of the superior colliculus. This area surrounding the cerebral aqueduct has been divided into subnuclei in the rat by Shipley et al. [9,84] and adapted for the hamster by Albers et al. [4]. The dorsal, ventral, and medial portions of the PAG contain a few large, intensely stained cells, as well as fibers, and terminals (Figs. 6F, 14) with a cluster of labeled cell bodies in the mid dorsal–ventral region medially (Fig. 14).

4. Discussion

4.1. Demonstration of enkephalin immunoreactivity in the hamster brain

This study demonstrates that enkephalin immunoreactive cells, fibers, and terminals are widely distributed within limbic areas, the basal ganglia, and the brainstem of the male Syrian hamster. Our observations are entirely consistent with those reported earlier for the hamster by Davis and his colleagues in the olfactory bulb [20] and nucleus of the tractus solitarius [18], as well as by McLean et al. [62] in the hippocampal formation and finally by Racz et al. [81] in their comparison of opioids in the hippocampus of four rodent species including the hamster. In addition, both the overall pattern and the specific location of enkephalin immunoreactive elements in the hamsters we have studied are similar to those reported for the rat in most brain areas [30,32,35,36,41–43,57,68,83,96]. Notable exceptions include the cingulate gyrus, lateral septum, and the VMH. Kuhar [53] reported met-enkephalin immunoreactive cell bodies throughout the lateral septum as well as the VMH of the rat. In comparison, we report that the hamster lateral septum contains met-enkephalin immunoreactive fibers and puncta only, while the pattern of staining for enkephalin cell bodies in the VMH is essentially confined to the lateral portion of the nucleus. Additionally, the cingulate gyrus of the rat contains enkephalinergic cells and fibers [34,61] while we did not identify any enkephalinergic elements in the cingulate gyrus of the hamster.

4.2. Technical considerations

4.2.1. Specificity of the antibodies—Several lines of evidence taken together indicate that the immunoreactivity described here is specific for enkephalin. Preabsorption of the met-enkephalin antibody with met-enkephalin, and of the leu-enkephalin antibody with leu-enkephalin, eliminated immunostaining. Further, there was no evidence for cross-reactivity of the met-enkephalin antibodies with leu-enkephalin and only a slight reactivity, or

diminution of staining, when the leu-enkephalin antibody was preincubated with met-enkephalin.

The neuroanatomical distribution of leu-enkephalin over-lapped that of met-enkephalin in all but one area (the main olfactory bulb), and all but one of the remaining areas contained less leu-enkephalin immunoreactivity, both within cells and in the number of immunostained cells. This quantitative difference also has been reported in studies employing radioimmunoassays for the enkephalins [37] and is consistent with the observation that postranslational processing of each preproenkephalin precursor results in four copies of met-enkephalin and one of leu-enkephalin [44,97]. The one area that contained more intensely labeled leu-enkephalin immunoreactive neurons than met-enkephalin immunoreactive cells was the posterointermediate subdivision of the BNST.

Finally, the distribution of enkephalin immunoreactivity described here is distinctly different from that of other endogenous opiates, including the distribution of prodynorphin as demonstrated with antibodies against dynorphin A, dynorphin B, and the C-terminus of the prodynorphin precursor molecule [70]. This is important because processing of prodynorphin can produce at least transient copies of leu-enkephalin [95,96].

4.2.2. Effects of colchicine on enkephalin production and sequestration—The antibodies used in this study for both met- and leu-enkephalin immunohistochemistry required the use of an axonal transport inhibitor for optimal visualization of enkephalin in cell bodies. A minimal dose of 50 μg of colchicine delivered intraventricularly was essential for staining somata above background levels.

A potential limitation of this technique was raised by the report of Cecatelli et al. [14] who observed an increase in enkephalin mRNA in the parvocellular paraventricular nucleus (PVN) of the rat hypothalamus 30 min following a bolus intraventricular injection of colchicine, with a return to normal levels 24 h after colchicine administration but increased in the hypothalamus and decreased in the pituitary after 48 h. Bayon et al. [10] also reported no change at either time point in the caudate/putamen, globus pallidus, preoptic area, or periaqueductal gray.

The results of these studies are consistent with the hypothesis that colchicine administration is a physiologically stressful treatment causing a transient and selective increase in enkephalin production in the PVN and metabolism and/or secretion in the pituitary, and that the subsequent action of colchicine is to prevent axonal transport of this newly produced enkephalin to the pituitary. These results indicate that the physiological actions of colchicine would limit its usefulness in attempting to determine “basal” levels of enkephalin in various areas of the brain and in quantitative comparisons of enkephalin content across brain regions.

The objective of the present study was simply to describe the neuroanatomical distribution of enkephalin-producing cells and their axonal projections. For this study, the important question is simply whether colchicine administration induces enkephalin production in neurons that normally produce no enkephalin. This would of course produce false positive

identification of enkephalin immunoreactive areas in the results reported above. We know of no evidence demonstrating this.

4.3. Implications for social behaviors

Most important for the purposes of this study is the observation of enkephalin immunoreactive cells and terminals in areas of the hamster brain that have been implicated previously in both sexual and agonistic behaviors in this species. Much of the circuitry that is critical for male hamster mating behavior was demonstrated with lesion, Fos immunohistochemistry and tract tracing studies. The circuitry for male hamster agonistic behavior has been derived with the same techniques and with data obtained from injections of arginine vasopressin (AVP) into brain regions critical for agonistic behavior in this species. Fig. 15 is a summary diagram of enkephalinergic neuronal distribution (reported in this study) in areas of the hamster brain in which previous studies have reported that lesions cause a deficit in male/female mating (Fig. 15A) [21,45,54–56,59,69,73,79,82] and brain regions in which lesions [7,8,12,33,39,59,88,90] or AVP injections [7,8] have been shown to modulate aggressive behavior (Fig. 15C). The results of previous Fos studies are also represented in Fig. 15, which illustrates specific cell groups where behaviorally induced increases in Fos protein suggest that either mating (Fig. 15A) or agonistic encounters (Fig. 15C), or both, increase activity of the neurons [46,47,49]. For comparison, Fig. 15B illustrates enkephalin immunoreactive neurons, fibers and/or terminals that are located within this social behavior circuitry as demonstrated in the present study.

In several of the areas illustrated in Fig. 15, the distribution of enkephalin containing cell bodies corresponds well with that of neurons that increase Fos production following agonistic behavior but not after mating. These nuclei include the BNSTal, the AH, the medial PVN, and the lateral VMH [47]. Although no studies have specifically explored the role of enkephalin in aggression of Syrian hamsters, other endogenous opiates have been implicated. For example, cell bodies immunoreactive for endomorphin-1, an endogenous opiate shown to block the expression of conditioned defeat [98], were recently demonstrated in the AH, PVN, and VMH of the Syrian hamster. In the dorsal PAG where increases in Fos immunoreactive cells have been observed after aggression in male hamsters [47], we find primarily enkephalin immunoreactive fibers and terminals. The potentiation of the excitatory action of NMDA in the periaqueductal gray by the opioid receptor agonist, DAMGO [52] suggests that the enkephalin terminals that we observe in the dorsal PAG may play a role in the activation of Fos immunoreactive neurons observed following agonistic behavior in the hamster.

Finally, in the BNST, enkephalin immunoreactive cell bodies are observed in areas that increase Fos production after either mating or aggression (anteromedial, posteromedial and posterointermediate subdivisions). Although this may reflect overlapping, but separate, functional populations of cells, it is also possible that some of these neurons have a more general, but nonetheless important, role in controlling the level of arousal in the male hamster during social behavior [47].

At present, direct evidence that enkephalin contributes to the regulation of social behaviors in hamster does not exist. However, there is evidence indicating that opioids are crucial for

female sexual behavior in the rat. Lordosis, a hormone-dependent mating posture displayed by sexually receptive female rodents during mating, is regulated by opioids [1,2,6,27,77,94]. These effects of opioids are site-dependent [75–77,86,87], dose-specific [76,77,86,99–101], and hormone-sensitive [1,2,91–93]. This report of the distribution of enkephalins in the hamster provides a framework for investigations of corresponding questions on the role of enkephalins in this species.

Nomenclature

ac	anterior commissure
AcbC	nucleus accumbens, core
AcbSh	nucleus accumbens, shell
acp	posterior limb of the anterior commissure
ACo	anterior cortical nucleus of the amygdala
ADPN	anterodorsal preoptic nucleus
AH	anterior hypothalamus
AHi	amygdalohippocampal area
AI	agranular insular cortex
alac	anterior limb of the anterior commissure
AMe	medial nucleus of the amygdala
AONp	anterior olfactory nucleus, posterior
Apir	amygdalopiriform transition area
ARC	arcuate nucleus
AVPV	anteroventral periventricular nucleus
Au	primary auditory cortex
BLa	anterior basolateral nucleus of the amygdala
BLp	posterior basolateral nucleus of the amygdala
BM	basomedial nucleus of the amygdala
BNSTal	bed nucleus of the stria terminalis, anterolateral
BNSTam	bed nucleus of the stria terminalis, anteromedial
BNSTav	bed nucleus of the stria terminalis, anteroventral
BNSTpi	bed nucleus of the stria terminalis, posterointermediate
BNSTpl	bed nucleus of the stria terminalis, posterolateral
BNSTpm	bed nucleus of the stria terminalis, posteromedial
CA	cerebral aqueduct

CA1	cornu ammonus, region 1
CA2	cornu ammonus, region 2
CA3	cornu ammonus, region 3
Ce	central nucleus of the amygdala
Cg	cingulate gyrus
Cg1	cingulate cortex, area 1
CP	caudate, putamen
cp	cerebral peduncle
DG	dentate gyrus
DGh	dentate gyrus, hilus
DMH	dorsomedial hypothalamic nucleus
DTT	dorsal tenia tecta
EC	entorhinal cortex
En	endopiriform nucleus
f	fornix
fi	fimbria of hippocampus
frf	fasciculus retroflexus
FP	frontal pole
FStr	fundus striati
GI	granular insular cortex
GP	globus pallidus
HLNDB	diagonal band of Broca, horizontal limb
ic	internal capsule
ICj	island of Calleja
ICjM	island of Calleja, magna
IL	infralimbic cortex
III	third ventricle
IPN	interpeduncular nucleus
La	lateral amygdaloid nucleus, anterior
LGN	lateral geniculate nucleus
lot	lateral olfactory tract
Lp	lateral amygdaloid nucleus, posterior

LPOA	lateral preoptic area
LSd	lateral septum, dorsal
LSi	lateral septum, intermediate
LSv	lateral septum, ventral
LV	lateral ventricle
M	motor cortex
M1	primary motor cortex
M2	secondary motor cortex
Me	medial nucleus of the amygdala
MeAD	medial nucleus of the amygdala, anterodorsal
MeAV	medial nucleus of the amygdala, anteroventral
MePD	medial nucleus of the amygdala, posterodorsal
MePV	medial nucleus of the amygdala, posteroventral
MePO	median preoptic nucleus
MGN	medial geniculate nucleus
MI	massa intercalata
MO	medial orbital cortex
MPN	medial preoptic nucleus
MPNmag	medial preoptic nucleus, magnocellular
MPOA	medial preoptic area
MS	medial septum
mt	mammilothalamic tract
NAOT	nucleus of the anterior olfactory tract
NLOT	nucleus of the lateral olfactory tract
oc	optic chiasm
ot	optic tract
OVLT	organum vasculosum
PAG	periaqueductal gray
pc	posterior commissure
Pir	piriform cortex
PLCo	posterior lateral cortical nucleus of the amygdala
PMCo	posterior medial cortical nucleus of the amygdala

PMD	dorsal premammillary nucleus
PMV	ventral premammillary nucleus
POC	primary olfactory cortex
PrL	prelimbic cortex
PT	parataenial nucleus
PVN	paraventricular nucleus of the hypothalamus
RN	red nucleus
RS	retrosplenial cortex
S	subiculum
S1	primary somatosensory cortex
S2	secondary somatosensory cortex
SC	superior colliculus
SCN	suprachiasmatic nucleus
SL	semilunar nucleus
sm	stria medullaris
SNc	substantia nigra, pars reticulata
SNr	substantia nigra, pars compacta
SON	supraoptic nucleus
st	stria terminalis
TT	tenia tecta
Tu	olfactory tubercle
Vi	visual cortex
VMH	ventromedial nucleus of the hypothalamus
VP	ventral pallidum
VTA	ventral tegmental area
VTT	ventral tenia tecta
ZI	zona incerta

References

1. Acosta-Martinez M, Etgen AM. Activation of mu-opioid receptors inhibits lordosis behavior in estrogen and progesterone-primed female rats. Horm. Behav. 2002; 41:88–100. [PubMed: 11863387]
2. Acosta-Martinez M, Etgen AM. The role of delta-opioid receptors in estrogen facilitation of lordosis behavior. Behav. Brain Res. 2002; 136:93–102. [PubMed: 12385794]

3. Agmo A, Gomez M, Irazabal Y. Enkephalinase inhibition facilitates sexual behavior in the male rat. Pharmacol. Biochem. Behav. 1994; 47:771–778. [PubMed: 8029244]
4. Albers HE, Hennessey AC, Whitman DC. Vasopressin and the regulation of hamster social behavior. Ann. N.Y. Acad. Sci. 1992; 652:227–242. [PubMed: 1626831]
5. Asmus SE, Kincaid AE, Newman SW. A species-specific population of tyrosine hydroxylase-immunoreactive neurons in the medial amygdaloid nucleus of the Syrian hamster. Brain Res. 1992; 575:199–207. [PubMed: 1349252]
6. Bakker J, Kelliher KR, Baum MJ. Mating induces gonadotropin-releasing hormone neuronal activation in anosmic female ferrets. Biol. Reprod. 2001; 64:1100–1105. [PubMed: 11259255]
7. Bamshad M, Albers HE. Neural circuitry controlling vasopressin-stimulated scent marking in Syrian hamsters (*Mesocricetus auratus*). J. Comp. Neurol. 1996; 369:252–263. [PubMed: 8726998]
8. Bamshad M, Karom M, Pallier P, Albers HE. Role of the central amygdala in social communication in Syrian hamsters (*Mesocricetus auratus*). Brain Res. 1997; 744:15–22. [PubMed: 9030408]
9. Bandler R, Shipley MT. Columnar organization in the midbrain periaqueductal gray: modules for emotional expression? Trends Neurosci. 1994; 17:379–389. (published erratum appears in Trends Neurosci. 1994 Nov.;17(11):445, see comments). [PubMed: 7817403]
10. Bayon A, Koda L, Battenberg E, Bloom FE. Redistribution of endorphin and enkephalin immunoreactivity in the rat brain and pituitary after in vivo treatment with colchicine or cytochalasin B. Brain Res. 1980; 183:103–111. [PubMed: 6153550]
11. Boyer PA, Trembleau A, Leviel V, Arluison M. Effects of intranigral injections of colchicine on the expression of some neuropeptides in the rat forebrain: an immunohistochemical and in situ hybridization study. Brain Res. Bull. 1994; 33:541–560. [PubMed: 7514485]
12. Bunnell BN, Sodetz FJ Jr, Shalloway DI. Amygdaloid lesions and social behavior in the golden hamster. Physiol. Behav. 1970; 5:153–161. [PubMed: 5535792]
13. Callard GV, Hoffman RA, Petro Z, Ryan KJ. In vitro aromatization and other androgen transformations in the brain of the hamster (*Mesocricetus auratus*). Biol. Reprod. 1979; 21:33–38. [PubMed: 486644]
14. Ceccatelli S, Cortes R, Hokfelt T. Effect of reserpine and colchicine on neuropeptide mRNA levels in the rat hypothalamic paraventricular nucleus. Brain Res. Mol. Brain Res. 1991; 9:57–69. [PubMed: 1850078]
15. Coolen LM, Wood RI. Bidirectional connections of the medial amygdaloid nucleus in the. J. Comp. Neurol. 1998; 399:189–209. [PubMed: 9721903]
16. Coolen LM, Wood RI. Testosterone stimulation of the medial preoptic area and medial amygdala in the control of male hamster sexual behavior: redundancy without amplification. Behav. Brain Res. 1999; 98:143–153. [PubMed: 10210530]
17. Daenen EW, Wolterink G, Gerrits MA, Van Ree JM. The effects of neonatal lesions in the amygdala or ventral hippocampus on social behaviour later in life. Behav. Brain Res. 2002; 136:571–582. [PubMed: 12429419]
18. Davis B, Kream R. Distribution of tachykinin- and opioid-expressing neurons in the hamster solitary nucleus: an immuno-and in situ hybridization histochemical study. Brain Res. 1993; 616:6–16. [PubMed: 7689413]
19. Davis BJ, Macrides F, Youngs WM, Schneider SP, Rosene DL. Efferents and centrifugal afferents of the main and accessory olfactory bulbs in the hamster. Brain Res. Bull. 1978; 3:59–72. [PubMed: 75756]
20. Davis B, Burd G, Macrides F. Localization of methionineen-kephalin, substance P, and somatostatin immunoreactivities in the main olfactory bulb of the hamster. J. Comp. Neurol. 1982; 204:377–383. [PubMed: 6174555]
21. DeBold JF, Malsbury CW. Inhibition of sexual receptivity after intracranial cycloheximide infusions in female hamsters. Brain Res. Bull. 1983; 11:633–636. [PubMed: 6661669]
22. Delville Y, De Vries GJ, Ferris CF. Neural connections of the anterior hypothalamus and agonistic behavior in golden hamsters. Brain Behav. Evol. 2000; 55:53–76. [PubMed: 10838477]
23. Devor M, Murphy MR. The effect of peripheral olfactory blockade on the social behavior of the male golden hamster. Behav. Biol. 1973; 9:31–42. [PubMed: 4738710]

24. Diaz JL, Asai M. Dominant mice show much lower concentrations of methionine-enkephalin in brain tissue than subordinates: cause or effect? Behav. Brain Res. 1990; 39:275–280. [PubMed: 2244973]
25. Ferris CF, Gold L, De Vries GJ, Potegal M. Evidence for a functional and anatomical relationship between the lateral septum and the hypothalamus in the control of flank marking behavior in Golden hamsters. J. Comp. Neurol. 1990; 293:476–485. [PubMed: 2324325]
26. Fiber JM, Adames P, Swann JM. Pheromones induce c-fos in limbic areas regulating male hamster mating behavior. NeuroReport. 1993; 4:871–874. [PubMed: 8369476]
27. Forsberg G, Bednar I, Eneroth P, Sodersten P. Naloxone reverses post-ejaculatory inhibition of sexual behaviour in female rats. J. Endocrinol. 1987; 113:429–434. [PubMed: 2957453]
28. Gomez DM, Newman SW. Medial nucleus of the amygdala in the adult Syrian hamster: a quantitative Golgi analysis of gonadal hormonal regulation of neuronal morphology. Anat. Rec. 1991; 231:498–509. [PubMed: 1793177]
29. Gomez DM, Newman SW. Differential projections of the anterior and posterior regions of the medial amygdaloid nucleus in the Syrian hamster. J. Comp. Neurol. 1992; 317:195–218. [PubMed: 1573064]
30. Gramsch C, Hollt V, Mehraein P, Pasi A, Herz A. Regional distribution of methionine-enkephalin- and beta-endorphin-like immunoreactivity in human brain and pituitary. Brain Res. 1979; 171:261–270. [PubMed: 466443]
31. Gray T, Magnuson D. Peptide immunoreactive neurons in the amygdala and the bed nucleus of the stria terminalis project to the midbrain central gray in the rat. Peptides. 1992 May-Jun;13:451–460. [PubMed: 1381826]
32. Gros C, Lafon Cazal M, Dray F. Presence of substances immunoreactively related to enkephalin in an insect, *Locusta migratoria*. C. R. Acad. Sci. Hebd. Seances Acad. Sci., D. 1978; 287:647–650. [PubMed: 103643]
33. Hammond MA, Rowe FA. Medial preoptic and anterior hypothalamic lesions: influences on aggressive behavior in female hamsters. Physiol. Behav. 1976; 17:507–513. [PubMed: 1034941]
34. Harlan RE, Shivers BD, Romano GJ, Howells RD, Pfaff DW. Localization of preproenkephalin mRNA in the rat brain and spinal cord by in situ hybridization. J. Comp. Neurol. 1987; 258:159–184. [PubMed: 3584538]
35. Hughes J. Isolation of an endogenous compound from the brain with pharmacological properties similar to morphine. Brain Res. 1975; 88:295–308. [PubMed: 1148827]
36. Hughes J, Smith TW, Kosterlitz HW, Fothergill LA, Morgan BA, Morris HR. Identification of two related pentapeptides from the brain with potent opiate agonist activity. Nature. 1975; 258:577–580. [PubMed: 1207728]
37. Ikeda Y, Nakao K, Yoshimasa T, Yanaihara N, Numa S, Imura H. Existence of Met-enkephalin-Arg6-Gly7-Leu8 with Met-enkephalin, Leu-enkephalin and Met-enkephalin-Arg6-Phe7 in the brain of guinea pig, rat and golden hamster. Biochem. Biophys. Res. Commun. 1982; 107:656–662. [PubMed: 7126233]
38. Jang T, Singer AG, O'Connell RJ. Induction of c-fos in hamster accessory olfactory bulbs by natural and cloned aphrodisin. NeuroReport. 2001; 12:449–452. [PubMed: 11234744]
39. Janzen WB, Bunnell BN. Septal lesions and the recovery of function in the juvenile hamster. Physiol. Behav. 1976; 16:445–452. [PubMed: 986659]
40. Kevetter GA, Winans SS. Connections of the corticomedial amygdala in the golden hamster. II: efferents of the "olfactory amygdala". J. Comp. Neurol. 1981; 197:99–111. [PubMed: 6164703]
41. Khachaturian H, Lewis ME, Watson SJ. Immunocytochemical studies with antisera against leu-enkephalin and an enkephalin-precursor fragment (BAM-22P) in the rat brain. Life Sci. 1982; 31:1879–1882. [PubMed: 6759829]
42. Khachaturian H, Lewis ME, Watson SJ. Colocalization of proenkephalin peptides in rat brain neurons. Brain Res. 1983; 279:369–373. [PubMed: 6640353]
43. Khachaturian H, Lewis ME, Watson SJ. Enkephalin systems in diencephalon and brainstem of the rat. J. Comp. Neurol. 1983; 220:310–320. [PubMed: 6358277]

44. Kilpatrick DL, Howells RD, Noe M, Bailey LC, Udenfriend S. Expression of preproenkephalin-like mRNA and its peptide products in mammalian testis and ovary. Proc. Natl. Acad. Sci. U. S. A. 1985; 82:7467–7469. [PubMed: 3864164]
45. Kirn J, Floody OR. Differential effects of lesions in three limbic areas on ultrasound production and lordosis by female hamsters. Behav. Neurosci. 1985; 99:1142–1152. [PubMed: 3843544]
46. Kollack SS, Newman SW. Mating behavior induces selective expression of Fos protein within the chemosensory pathways of the male Syrian hamster brain. Neurosci. Lett. 1992; 143:223–228. [PubMed: 1436670]
47. Kollack-Walker S, Newman SW. Mating and agonistic behavior produce different patterns of Fos immunolabeling in the male Syrian hamster brain. Neuroscience. 1995; 66:721–736. [PubMed: 7644033]
48. Kollack-Walker S, Newman SW. Mating-induced expression of c-fos in the male Syrian hamster brain: role of experience, pheromones, and ejaculations. J. Neurobiol. 1997; 32:481–501. [PubMed: 9110260]
49. Kollack-Walker S, Watson SJ, Akil H. Social stress in hamsters: defeat activates specific neurocircuits. J. Neurosci. 1997; 17:8842–8855. [PubMed: 9348352]
50. Kollack-Walker S, Don C, Watson SJ, Akil H. Differential expression of c-fos mRNA within neurocircuits of male hamsters exposed to acute or chronic defeat. J. Neuroendocrinol. 1999; 11:547–559. [PubMed: 10444312]
51. Konig M, Zimmer AM, Steiner H, Holmes PV, Crawley JN, Brownstein MJ, Zimmer A. Pain responses, anxiety and aggression in mice deficient in pre-proenkephalin. Nature. 1996; 383:535–538. [PubMed: 8849726]
52. Kow LM, Commons KG, Ogawa S, Pfaff DW. Potentiation of the excitatory action of NMDA in ventrolateral periaqueductal gray by the mu-opioid receptor agonist, DAMGO. Brain Res. 2002; 935:87–102. [PubMed: 12062477]
53. Kuhar MJ. Histochemical localization of opiate receptors and opioid peptides. Fed. Proc. 1978; 37:153–157. [PubMed: 203493]
54. Lehman MN, Winans SS. Vomeronasal and olfactory pathways to the amygdala controlling male hamster sexual behavior: autoradiographic and behavioral analyses. Brain Res. 1982; 240:27–41. [PubMed: 7093718]
55. Lehman MN, Winans SS. Evidence for a ventral non-strial pathway from the amygdala to the bed nucleus of the stria terminalis in the male golden hamster. Brain Res. 1983; 268:139–146. [PubMed: 6305458]
56. Lehman MN, Winans SS, Powers JB. Medial nucleus of the amygdala mediates chemosensory control of male hamster sexual behavior. Science. 1980; 210:557–560. [PubMed: 7423209]
57. Mains RE, Eipper BA, Ling N. Common precursor to corticotropins and endorphins. Proc. Natl. Acad. Sci. U. S. A. 1977; 74:3014–3018. [PubMed: 197529]
58. Mak P, Callard GV. Characterization of estrogen receptors in the hamster brain. J. Steroid Biochem. 1985; 22:355–361. [PubMed: 3990285]
59. Malsbury CW, Kow LM, Pfaff DW. Effects of medial hypothalamic lesions on the lordosis response and other behaviors in remale golden hamsters. Physiol. Behav. 1977; 19:223–237. [PubMed: 607234]
60. Maragos WF, Newman SW, Lehman MN, Powers JB. Neurons of origin and fiber trajectory of amygdalofugal projections to the medial preoptic area in Syrian hamsters. J. Comp. Neurol. 1989; 280:59–71. [PubMed: 2918096]
61. McGinty JF, van der Kooy D, Bloom FE. The distribution and morphology of opioid peptide immunoreactive neurons in the cerebral cortex of rats. J. Neurosci. 1984; 4:1104–1117. [PubMed: 6143786]
62. McLean S, Rothman RB, Jacobson AE, Rice KC, Herkenham M. Distribution of opiate receptor subtypes and enkephalin and dynorphin immunoreactivity in the hippocampus of squirrel, guinea pig, rat, and hamster. J. Comp. Neurol. 1987; 255:497–510. [PubMed: 2880880]
63. Meisel, R.; Sachs, B. The physiology of male sexual behavior. In: Knobil, E.; Neill, JD., editors. The Physiology of Reproduction. New York: Raven Press; 1994. p. 3-105.

64. Miceli MO, van der Kooy D, Post CA, Della-Fera MA, Baile CA. Differential distributions of cholecystokinin in hamster and rat. Brain Res. 1987; 402:318–330. [PubMed: 3828799]
65. Morin LP, Blanchard J. Organization of the hamster paraventricular hypothalamic nucleus. J. Comp. Neurol. 1993; 332:341–357. [PubMed: 7687256]
66. Morin, LP.; Wood, RI. A Stereotaxic Atlas of the Golden Hamster Brain. San Diego, CA: Academic Press; 2001. 146, xv
67. Murphy MR, Schneider GE. Olfactory bulb removal eliminates mating behavior in the male golden hamster. Science. 1970; 167:302–304. [PubMed: 5409714]
68. Nakao K, Suda M, Sakamoto M, Yoshimasa T, Morii N, Ikeda Y, Yanaihara C, Yanaihara N, Numa S, Imura H. Leumorphin is a novel endogenous opioid peptide derived from preproenkephalin B. Biochem. Biophys. Res. Commun. 1983; 117:695–701. [PubMed: 6689399]
69. Nance DM, Myatt GA. Female sexual behavior in the golden hamster following kainic acid lesions in the lateral septal area. Brain Res. Bull. 1987; 19:751–754. [PubMed: 3440220]
70. Neal CR Jr, Newman SW. Prodynorphin peptide distribution in the forebrain of the Syrian hamster and rat: a comparative study with antisera against dynorphin A, dynorphin B, and the C-terminus of the prodynorphin precursor molecule. J. Comp. Neurol. 1989; 288:353–386. [PubMed: 2571622]
71. Neal CR Jr, Newman SW. Prodynorphin- and substance P-containing neurons project to the medial preoptic area in the male Syrian hamster brain. Brain Res. 1991; 546:119–131. [PubMed: 1713117]
72. Neal CR Jr, Swann JM, Newman SW. The colocalization of substance P and prodynorphin immunoreactivity in neurons of the medial preoptic area, bed nucleus of the stria terminalis and medial nucleus of the amygdala of the Syrian hamster. Brain Res. 1989; 496:1–13. [PubMed: 2478255]
73. Newman SW, Parfitt DB, Kollack-Walker S. Mating-induced c-fos expression patterns complement and supplement observations after lesions in the male Syrian hamster brain. Ann. N.Y. Acad. Sci. 1997; 807:239–259. [PubMed: 9071355]
74. Petrulis A, Johnston RE. Lesions centered on the medial amygdala impair scent-marking and sex-odor recognition but spare discrimination of individual odors in female golden hamsters. Behav. Neurosci. 1999; 113:345–357. [PubMed: 10357459]
75. Pfaus JG, Gorzalka BB. Opioids and sexual behavior. Neurosci. Biobehav. Rev. 1987; 11:1–34. [PubMed: 3554038]
76. Pfaus JG, Gorzalka BB. Selective activation of opioid receptors differentially affects lordosis behavior in female rats. Peptides. 1987; 8:309–317. [PubMed: 3035514]
77. Pfaus JG, Pendleton N, Gorzalka BB. Dual effect of morphiceptin on lordosis behavior: possible mediation by different opioid receptor subtypes. Pharmacol. Biochem. Behav. 1986; 24:1461–1464. [PubMed: 3014568]
78. Pohorecky LA, Skiandos A, Zhang X, Rice KC, Benjamin D. Effect of chronic social stress on delta-opioid receptor function in the rat. J. Pharmacol. Exp. Ther. 1999; 290:196–206. [PubMed: 10381776]
79. Powers JB, Newman SW, Bergondy ML. MPOA and BNST lesions in male Syrian hamsters: differential effects on copulatory and chemoinvestigatory behaviors. Behav. Brain Res. 1987; 23:181–195. [PubMed: 3555537]
80. Raab A, Seizinger BR, Herz A. Continuous social defeat induces an increase of endogenous opioids in discrete brain areas of the mongolian gerbil. Peptides. 1985; 6:387–391. [PubMed: 2866494]
81. Racz B, Fuzesi M, Halasy K. The hippocampal opioidergic system: a comparative immunocytochemical study in four rodents. Neurobiology (Bp.). 1998; 6:429–441. [PubMed: 10220778]
82. Raitiere MN, Garyfallou VT, Urbanski HF. Lesions in the anterior bed nucleus of the stria terminalis in Syrian hamsters block short-photoperiod-induced testicular regression. Biol. Reprod. 1997; 57:796–806. [PubMed: 9314583]
83. Roberts GW, Allen Y, Crow TJ, Polak JM. Immunocytochemical localization on neuropeptides in the fornix of rat, monkey and man. Brain Res. 1983; 263:151–155. [PubMed: 6188516]

84. Shipley MT, McLean JH, Behbehani MM. Heterogeneous distribution of neurotensin-like immunoreactive neurons and fibers in the midbrain periaqueductal gray of the rat. J. Neurosci. 1987; 7:2025–2034. [PubMed: 3302124]
85. Simerly RB, Swanson LW. Castration reversibly alters levels of cholecystokinin immunoreactivity within cells of three interconnected sexually dimorphic forebrain nuclei in the rat. Proc. Natl. Acad. Sci. U. S. A. 1987; 84:2087–2091. [PubMed: 3550806]
86. Sirinathsinghji DJ. Modulation of lordosis behavior of female rats by naloxone, beta-endorphin and its antiserum in the mesencephalic central gray: possible mediation via GnRH. Neuroendocrinology. 1984; 39:222–230. [PubMed: 6209590]
87. Sirinathsinghji DJ. Modulation of lordosis behaviour in the female rat by corticotropin releasing factor, beta-endorphin and gonadotropin releasing hormone in the mesencephalic central gray. Brain Res. 1985; 336:45–55. [PubMed: 2860950]
88. Sodetz FJ, Bunnell BN. Septal ablation and the social behavior of the golden hamster. Physiol. Behav. 1970; 5:79–88. [PubMed: 5538529]
89. Swann J, Rahaman F, Bijak T, Fiber J. The main olfactory system mediates pheromone-induced fos expression in the extended amygdala and preoptic area of the male Syrian hamster. Neuroscience. 2001; 105:695–706. [PubMed: 11516834]
90. Takahashi LK, Gladstone CD. Medial amygdaloid lesions and the regulation of sociosexual behavioral patterns across the estrous cycle in female golden hamsters. Behav. Neurosci. 1988; 102:268–275. [PubMed: 3365322]
91. Torii M, Kubo K. The effects of intraventricular injection of beta-endorphin on initial estrogen action to induce lordosis behavior. Physiol. Behav. 1994; 55:157–162. [PubMed: 8140161]
92. Torii M, Kubo K, Sasaki T. Differential effects of beta-endorphin and Met- and Leu-enkephalin on steroid hormone-induced lordosis in ovariectomized female rats. Pharmacol. Biochem. Behav. 1997; 58:837–842. [PubMed: 9408184]
93. Torii M, Kubo K, Sasaki T. Facilitatory and inhibitory effects of beta-endorphin on lordosis in female rats: relation to time of administration. Horm. Behav. 1999; 35:271–278. [PubMed: 10373339]
94. Vathy I, van der Plas J, Vincent PA, Etgen AM. Intracranial dialysis and microinfusion studies suggest that morphine may act in the ventromedial hypothalamus to inhibit female rat sexual behavior. Horm. Behav. 1991; 25:354–366. [PubMed: 1657761]
95. Watson SJ, Akil H. Recent studies on dynorphin and enkephalin precursor fragments in central nervous system. Adv. Biochem. Psychopharmacol. 1982; 33:35–42. [PubMed: 6127003]
96. Watson SJ, Khachaturian H, Akil H, Coy DH, Goldstein A. Comparison of the distribution of dynorphin systems and enkephalin systems in brain. Science. 1982; 218:1134–1136. [PubMed: 6128790]
97. Weisinger G. The transcriptional regulation of the preproenkephalin gene. Biochem. J. 1995; 307:617–629. [PubMed: 7741689]
98. Whitten RD, Jasnow AM, Albers HE, Martin-Schild S, Zadina JE, Huhman KL. The effects of endomorphin-1 on conditioned defeat in Syrian hamsters (*Mesocricetus auratus*). Brain Res. 2001; 914:74–80. [PubMed: 11578599]
99. Wiesner JB, Moss RL. Beta-endorphin suppression of lordosis behavior in female rats; lack of effect of peripherally-administered naloxone. Life Sci. 1984; 34:1455–1462. [PubMed: 6323904]
100. Wiesner JB, Moss RL. Behavioral specificity of beta-endorphin suppression of sexual behavior: differential receptor antagonism. Pharmacol. Biochem. Behav. 1986; 24:1235–1239. [PubMed: 3014564]
101. Wiesner JB, Dudley CA, Moss RL. Effect of beta-endorphin on sociosexual proclivity in a choice paradigm. Pharmacol. Biochem. Behav. 1986; 24:507–511. [PubMed: 2939466]
102. Winans SS, Powers JB. Olfactory and vomeronasal deafferentation of male hamsters: histological and behavioral analyses. Brain Res. 1977; 126:325–344. [PubMed: 861723]
103. Wood RI, Newman SW. Intracellular partitioning of androgen receptor immunoreactivity in the brain of the male Syrian hamster: effects of castration and steroid replacement. J. Neurobiol. 1993; 24:925–938. [PubMed: 8228970]

104. Wood RI, Newman SW. Mating activates androgen receptor-containing neurons in chemosensory pathways of the male Syrian hamster brain. Brain Res. 1993; 614:65–77. [PubMed: 8348332]

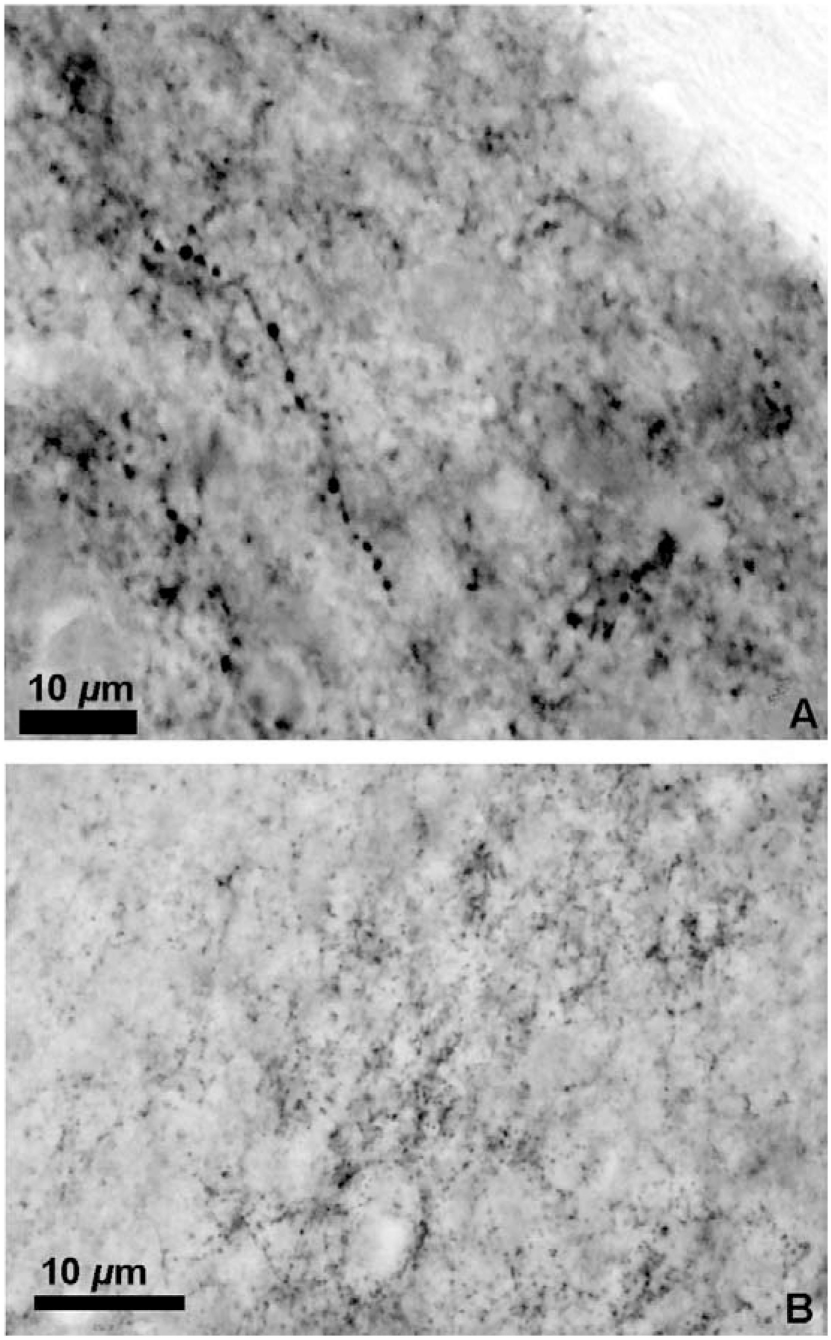

Fig. 1.

(A) Photomicrograph of a met-enkephalin immunoreactive fiber in the medial nucleus of the amygdala; (B) photomicrograph of the met-enkephalin immunoreactive puncta in the ventral lateral septum. Measure bar =10 μm for (A) and (B).

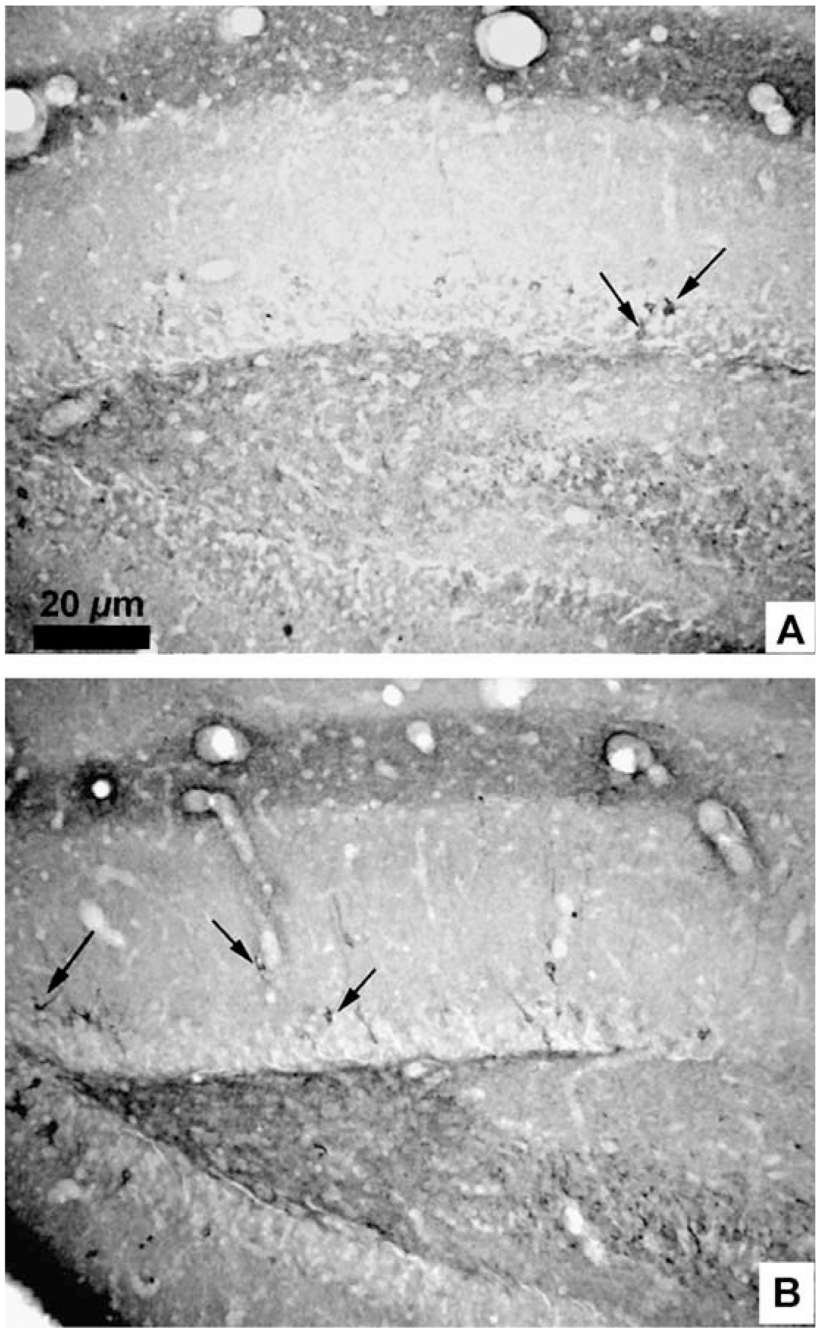

Fig. 2.

Photomicrographs of the dentate gyrus of the hippocampal formation after immunohistochemistry for leu-enkephalin (A) and met-enkephalin (B). Arrows indicate immunoreactive neurons. Measure bar =20 μm for (A) and (B).

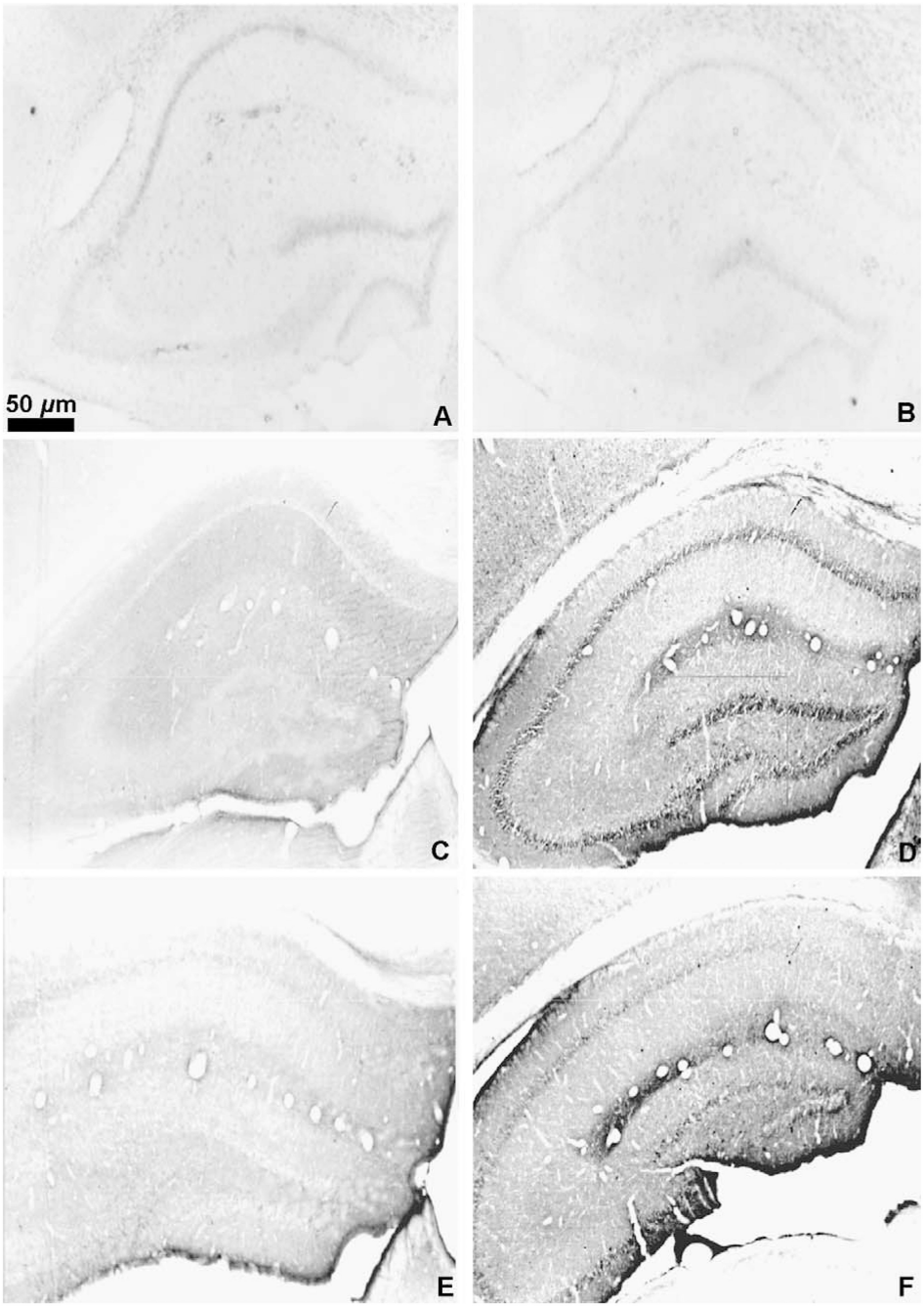

Fig. 3.

Photomicrographs of the hippocampal formation. (A) Immunohistochemistry for met-enkephalin with omission of the primary antibody; (B) Immunohistochemistry for met-enkephalin with omission of the secondary antibody; (C) Preabsorption of the met-enkephalin antibody with 10 μM met-enkephalin. (D) Immunohistochemistry for met-enkephalin after preabsorption with 75 μM leu-enkephalin; (E) Preabsorption of the leu-enkephalin antibody with 10 μM leu-enkephalin. (F) Preabsorption of the leu-enkephalin antibody with 75 μM met-enkephalin. In (A), (B), (C), and (E), photos were taken with dark

field microscopy, images were imported into the graphics program Adobe Photoshop, and "inverted" to allow visualization of the anatomy of the unstained sections.

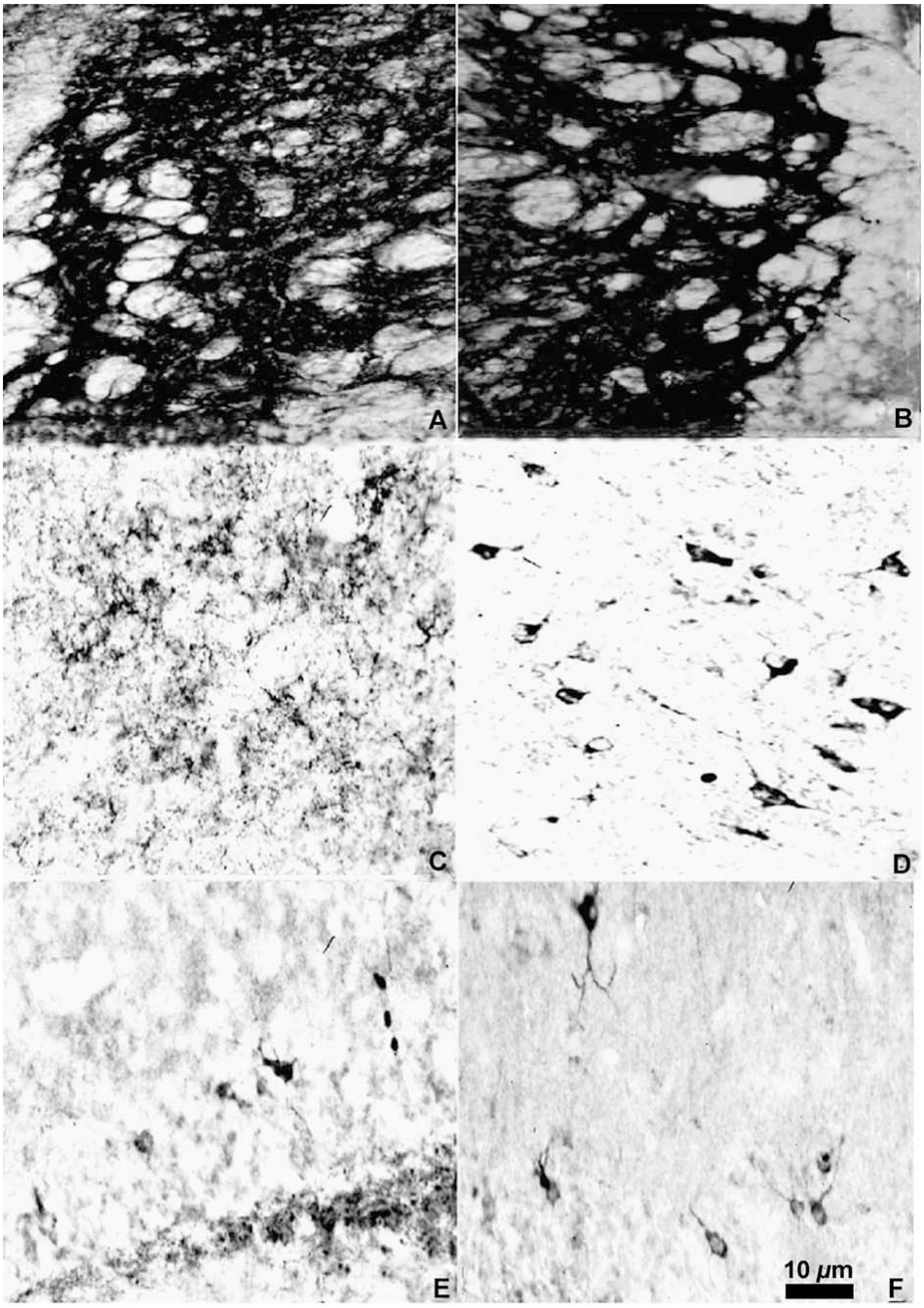

Fig. 4.

Photomicrograph of met-enkephalin immunoreactivity in the globus pallidus (A) and (B), the periaqueductal gray (C) and (D) and the dentate gyrus of the hippocampal formation (E) and (F) in animals without colchicine pretreatment (A), (C), and (E) or with 200 μg of colchicine (B), (D), and (F). Measure bar =10 μm for all photomicrographs.

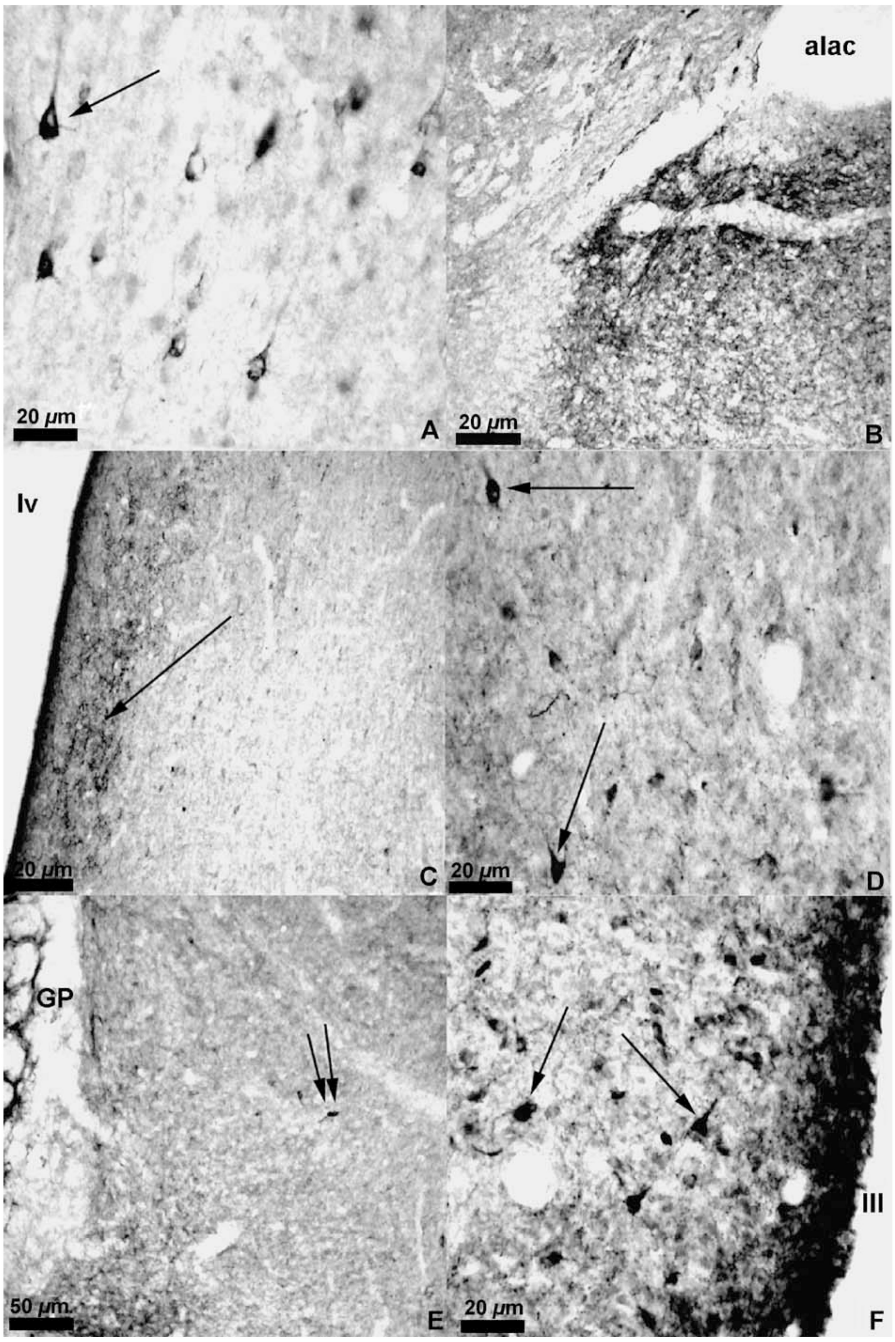

Fig. 5.

Photomicrographs of met-enkephalin immunoreactive cells in the cortex (A), medial septum (D), the bed nucleus of the stria terminalis (E) (the heavily labeled fibers of the globus pallidus are seen on the left), and the medial preoptic nucleus (F). Photomicrographs of enkephalin immunoreactive fibers and puncta in the ventral pallidum (B) and lateral septum (C).

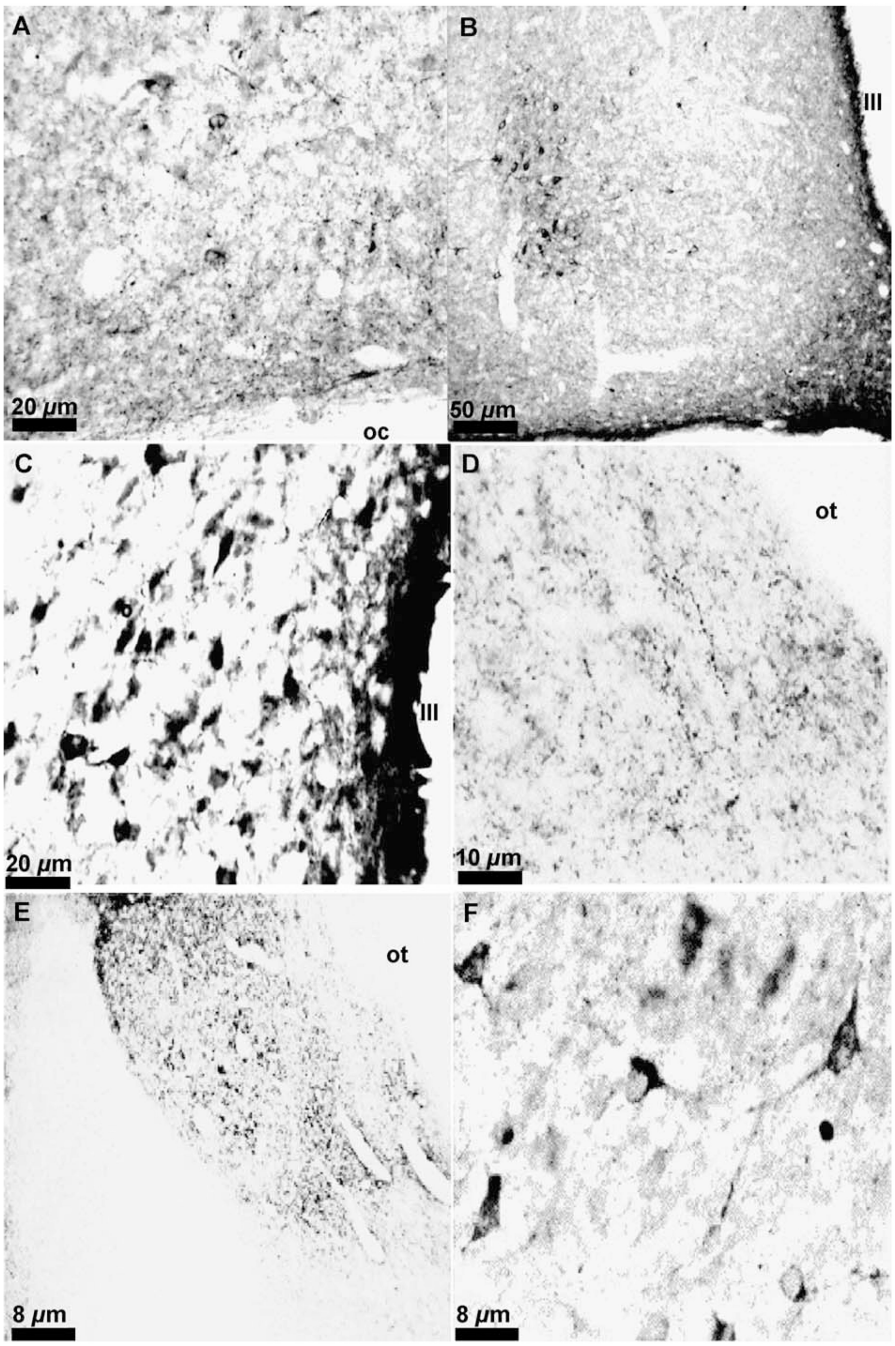

Fig. 6.

Photomicrographs of met-enkephalin immunoreactive cells in the anterior hypothalamic nucleus (A), ventromedial hypothalamic nucleus (B), and paraventricular nucleus (C) as well as photomicrographs of met-enkephalin immunoreactive fibers and puncta in the medial nucleus of the amygdala (D) and central nucleus of the amygdala (E). Large enkephalin immunoreactive cells are also found in the periaqueductal gray (F).

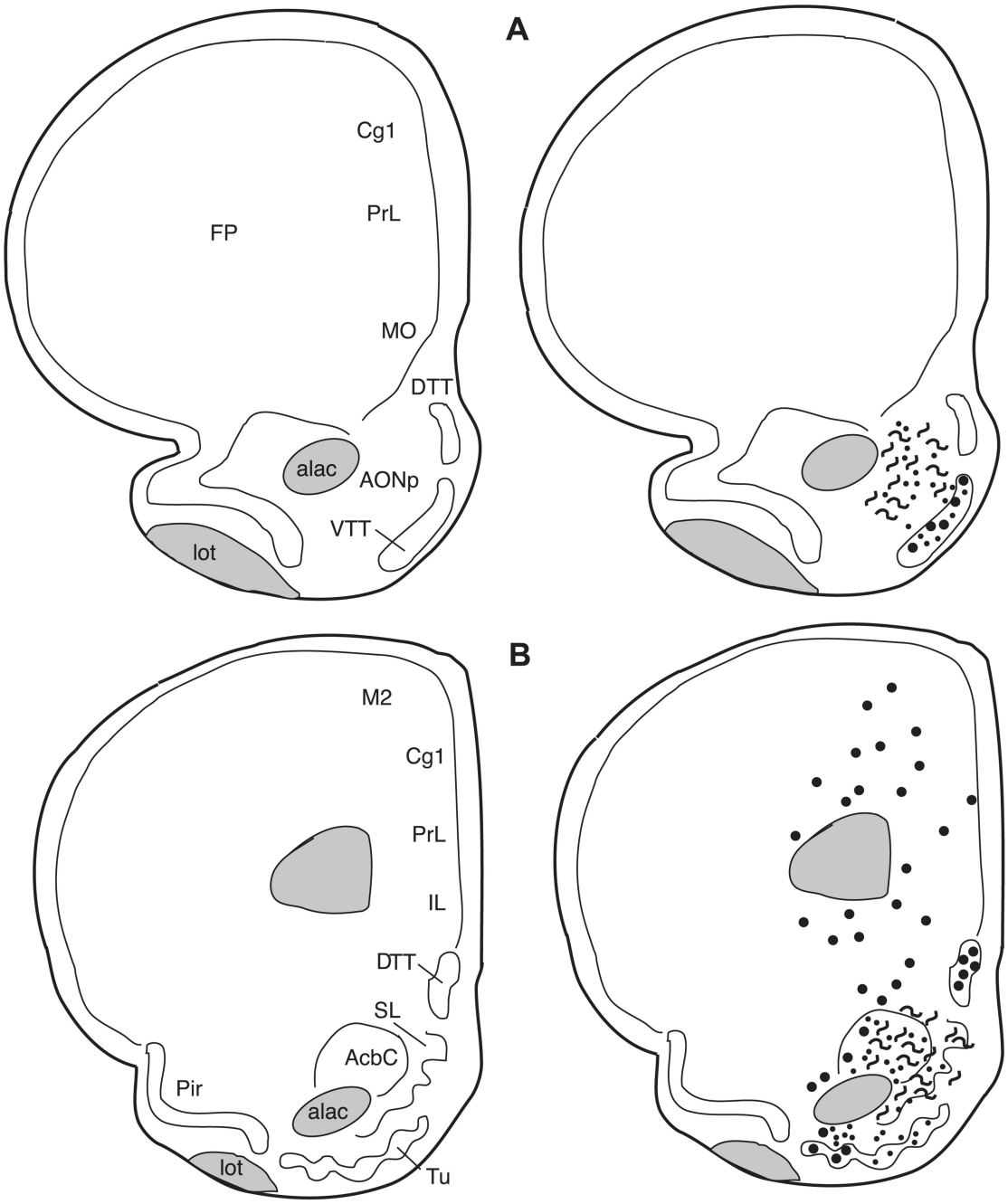

Fig. 7.

The distribution of enkephalin immunoreactive cells, fibers, and terminals throughout the forebrain and midbrain of the male Syrian hamster. The circles represent enkephalin immunoreactive cell bodies, the squiggly lines represent enkephalin immunoreactive fibers, and the dots represent enkephalin immunoreactive terminal fields. The mapping illustrated here represents a composite of the most consistently labeled regions from six colchicine-treated brains and two non-colchicine-treated brains.

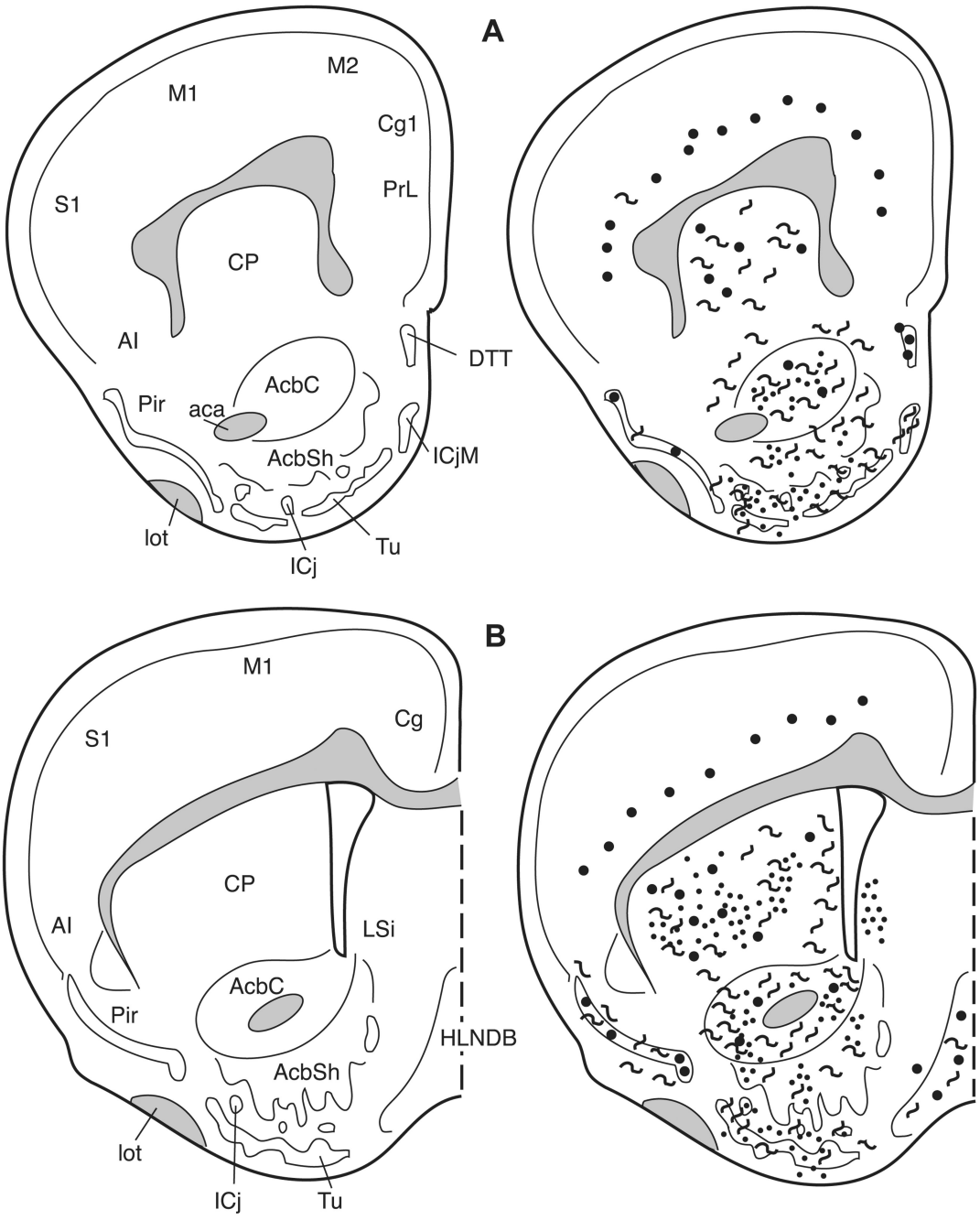

Fig. 8.

The distribution of enkephalin immunoreactive cells, fibers, and terminals throughout the forebrain and midbrain of the male Syrian hamster. The circles represent enkephalin immunoreactive cell bodies, the squiggly lines represent enkephalin immunoreactive fibers, and the dots represent enkephalin immunoreactive terminal fields. The mapping illustrated here represents a composite of the most consistently labeled regions from six colchicine-treated brains and two non-colchicine-treated brains.

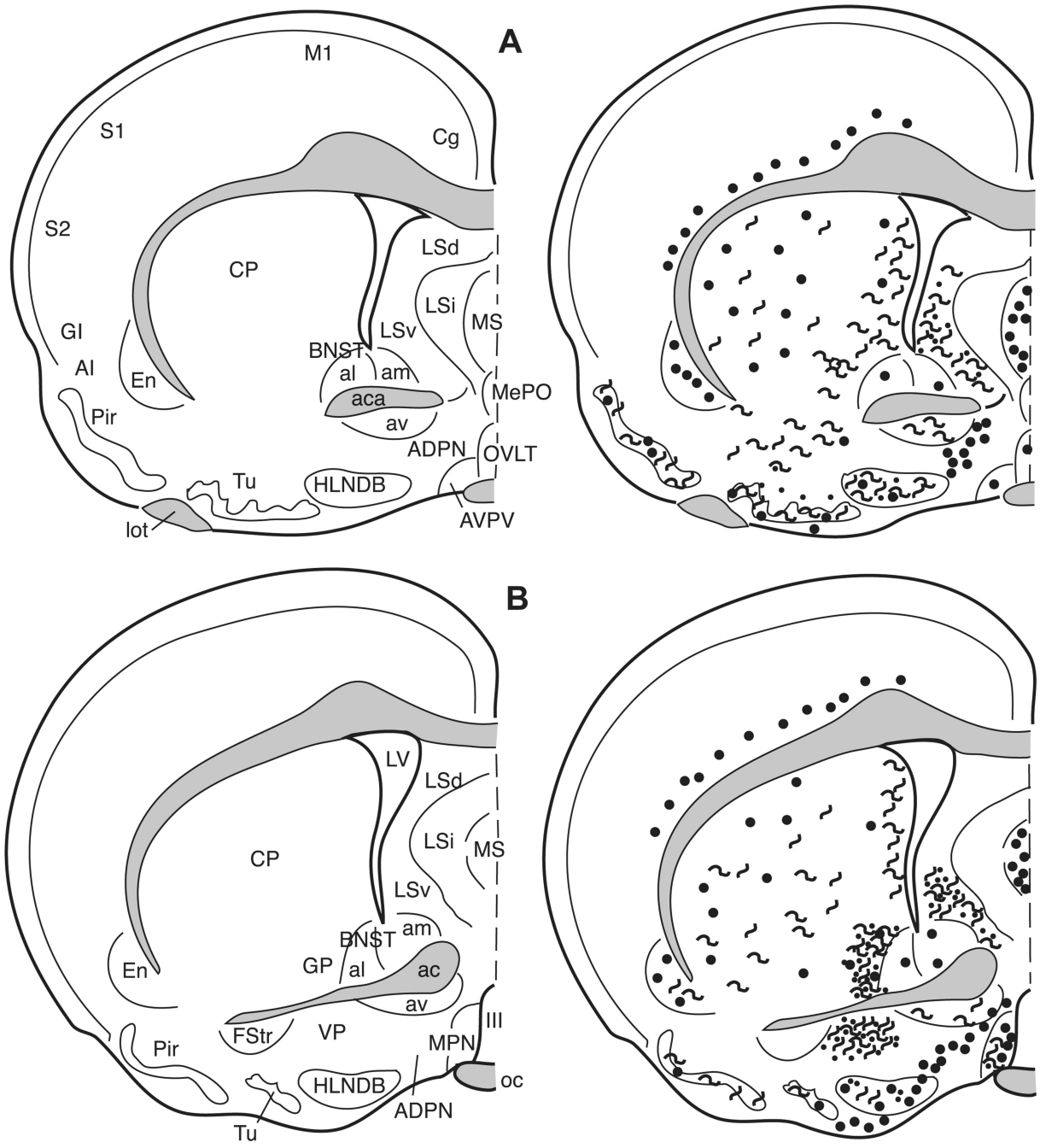

Fig. 9.

The distribution of enkephalin immunoreactive cells, fibers, and terminals throughout the forebrain and midbrain of the male Syrian hamster. The circles represent enkephalin immunoreactive cell bodies, the squiggly lines represent enkephalin immunoreactive fibers, and the dots represent enkephalin immunoreactive terminal fields. The mapping illustrated here represents a composite of the most consistently labeled regions from six colchicine-treated brains and two non-colchicine-treated brains.

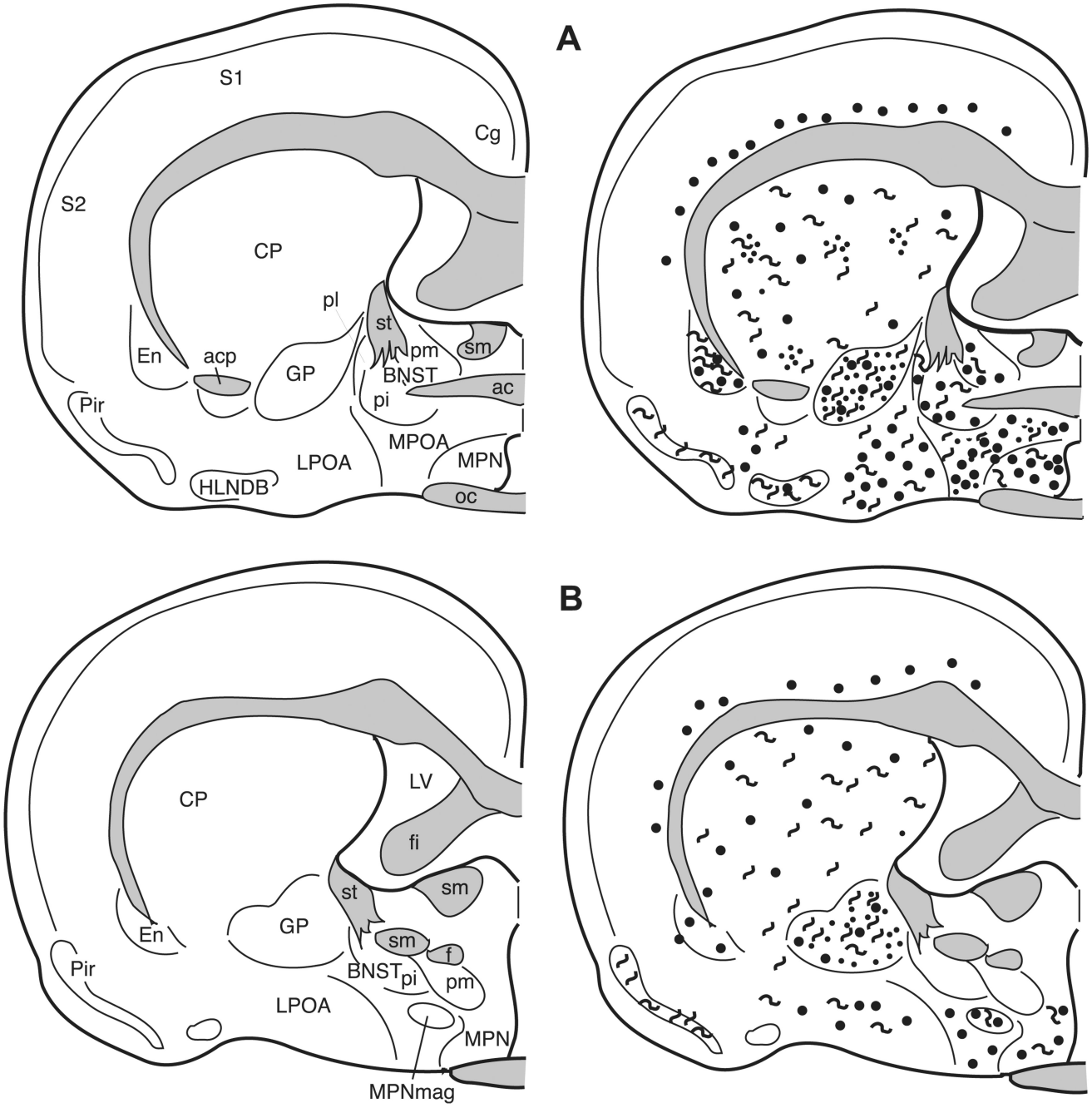

Fig. 10.

The distribution of enkephalin immunoreactive cells, fibers, and terminals throughout the forebrain and midbrain of the male Syrian hamster. The circles represent enkephalin immunoreactive cell bodies, the squiggly lines represent enkephalin immunoreactive fibers, and the dots represent enkephalin immunoreactive terminal fields. The mapping illustrated here represents a composite of the most consistently labeled regions from six colchicine-treated brains and two non-colchicine-treated brains.

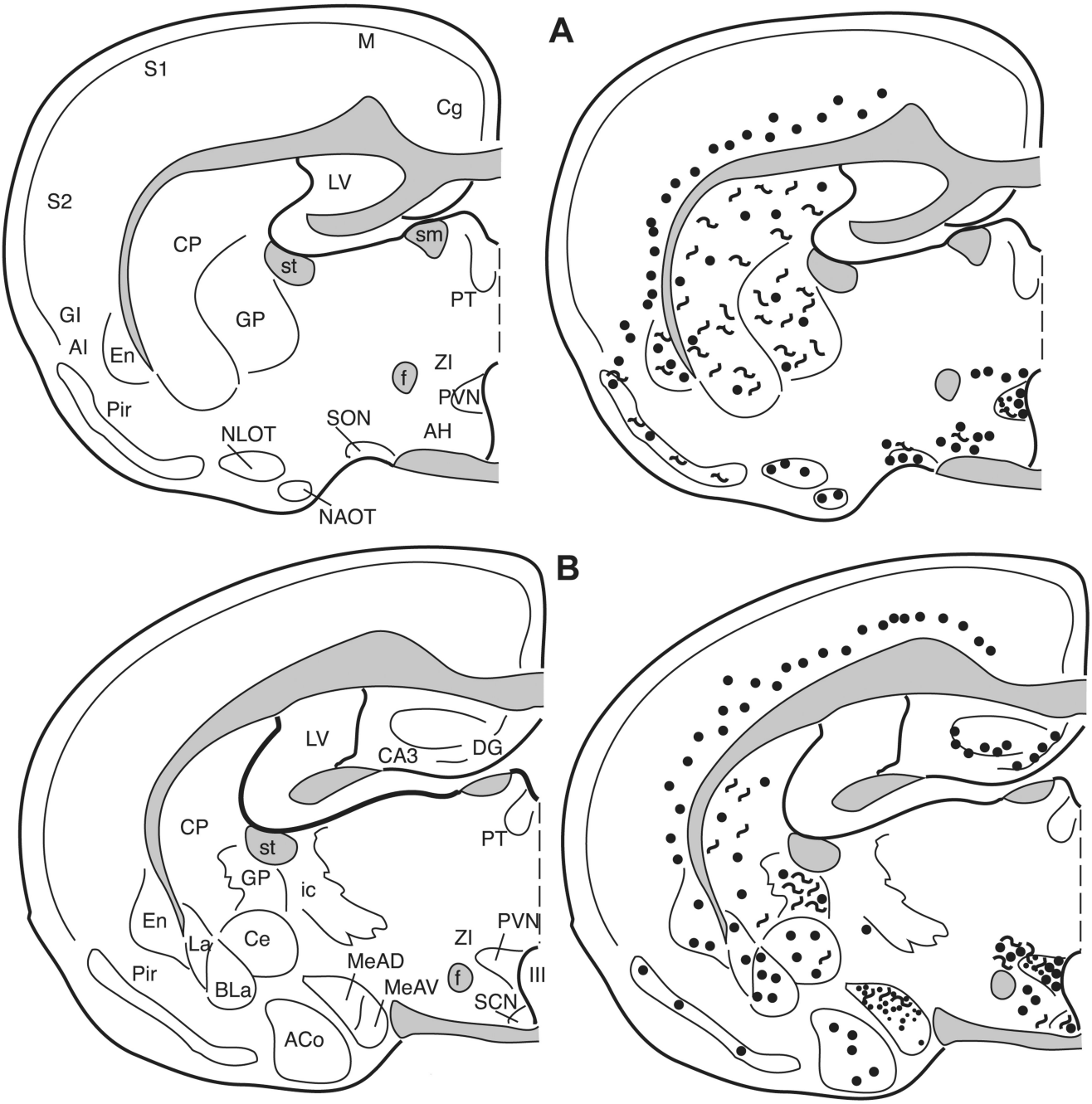

Fig. 11.

The distribution of enkephalin immunoreactive cells, fibers, and terminals throughout the forebrain and midbrain of the male Syrian hamster. The circles represent enkephalin immunoreactive cell bodies, the squiggly lines represent enkephalin immunoreactive fibers, and the dots represent enkephalin immunoreactive terminal fields. The mapping illustrated here represents a composite of the most consistently labeled regions from six colchicine-treated brains and two non-colchicine-treated brains.

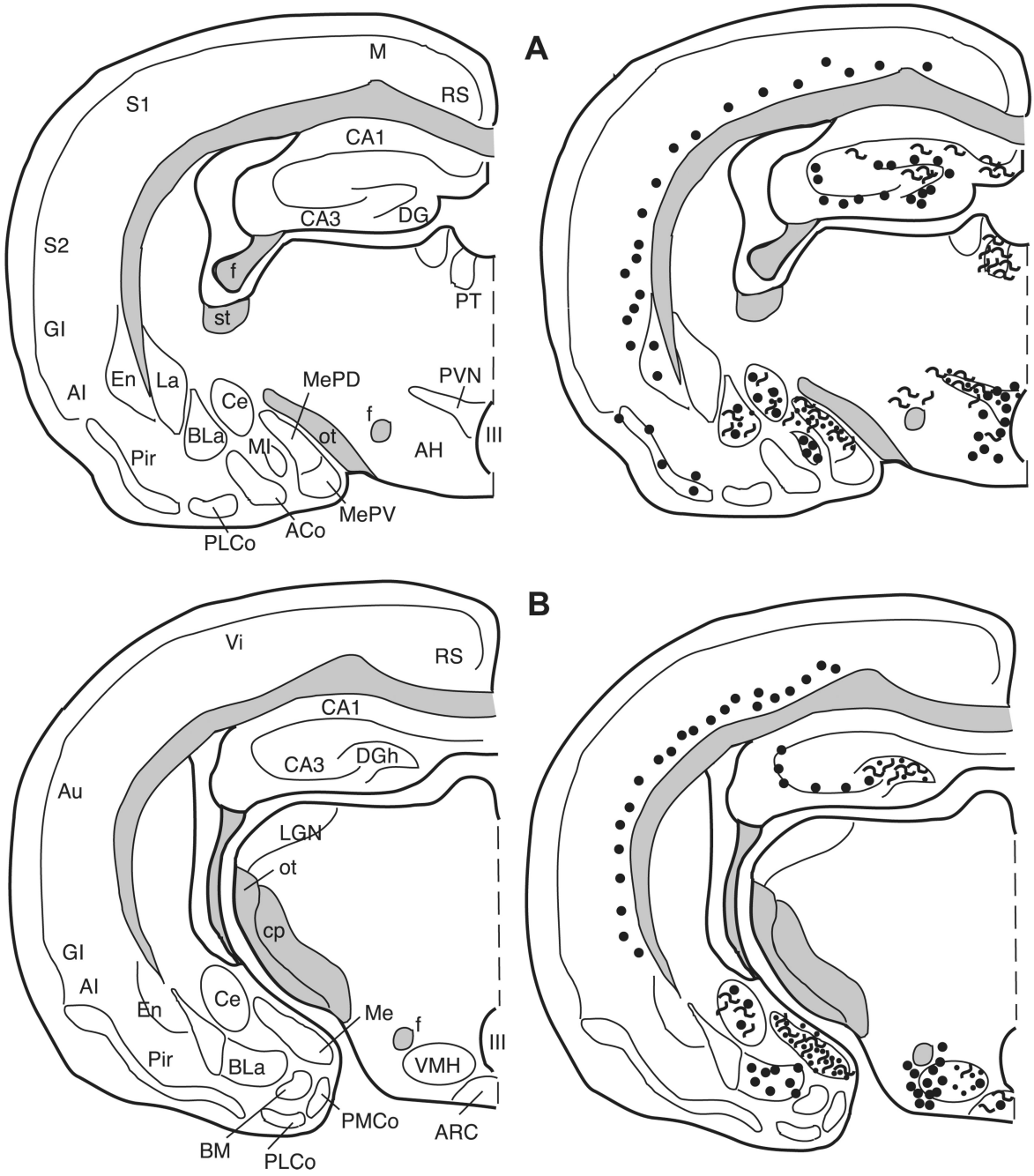

Fig. 12.

The distribution of enkephalin immunoreactive cells, fibers, and terminals throughout the forebrain and midbrain of the male Syrian hamster. The circles represent enkephalin immunoreactive cell bodies, the squiggly lines represent enkephalin immunoreactive fibers, and the dots represent enkephalin immunoreactive terminal fields. The mapping illustrated here represents a composite of the most consistently labeled regions from six colchicine-treated brains and two non-colchicine-treated brains.

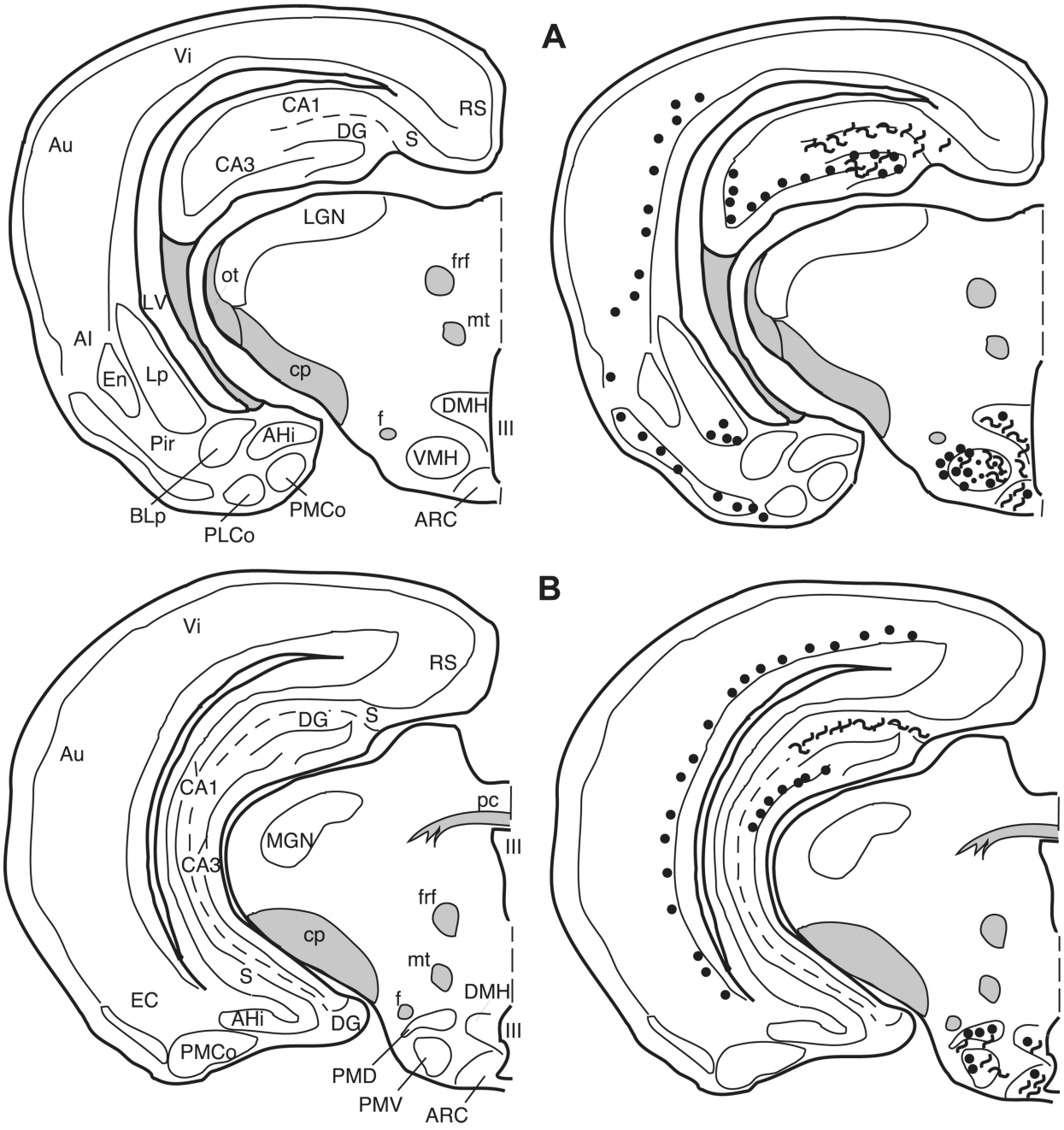

Fig. 13.

The distribution of enkephalin immunoreactive cells, fibers, and terminals throughout the forebrain and midbrain of the male Syrian hamster. The circles represent enkephalin immunoreactive cell bodies, the squiggly lines represent enkephalin immunoreactive fibers, and the dots represent enkephalin immunoreactive terminal fields. The mapping illustrated here represents a composite of the most consistently labeled regions from six colchicine-treated brains and two non-colchicine-treated brains.

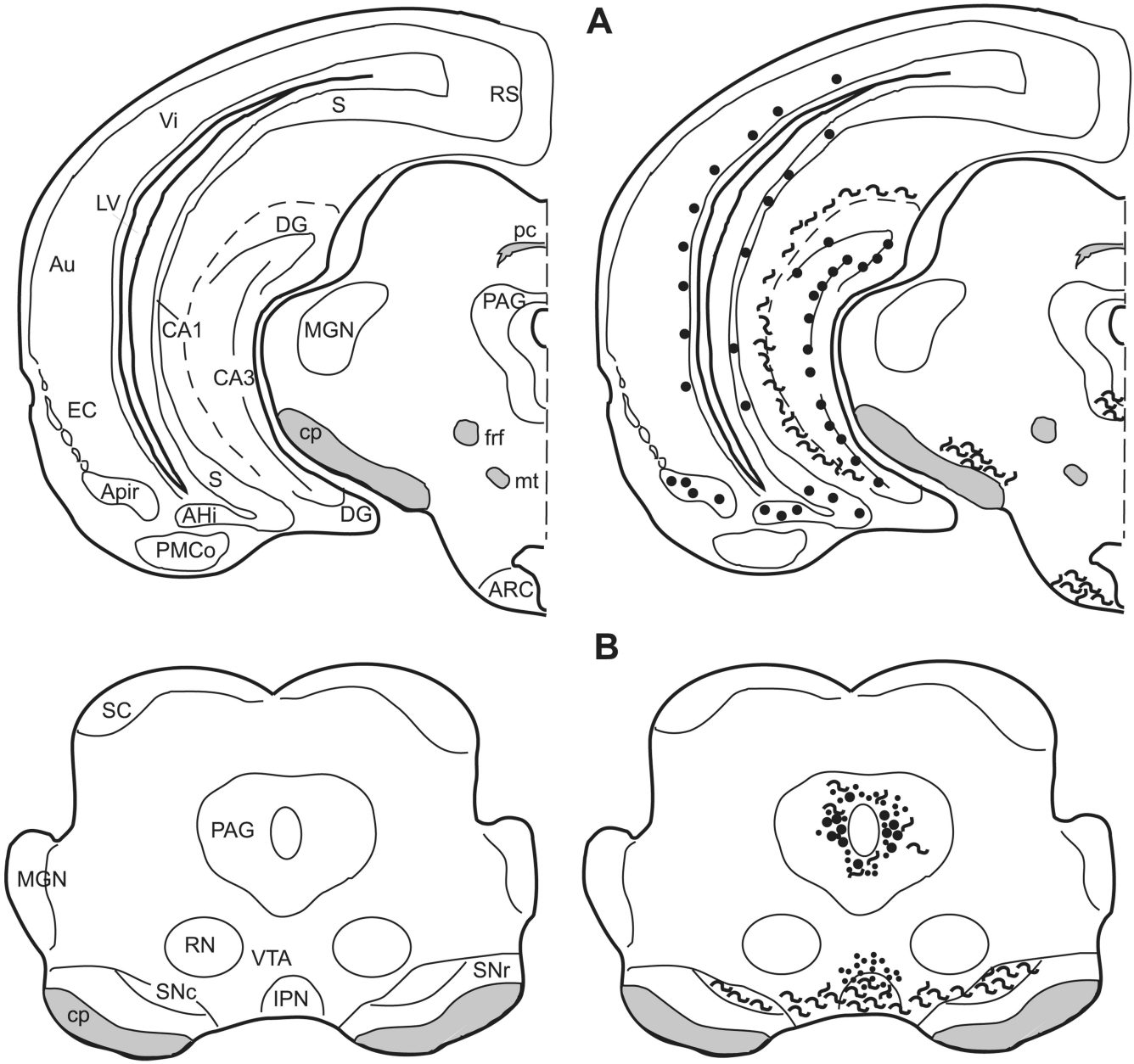

Fig. 14.

The distribution of enkephalin immunoreactive cells, fibers, and terminals throughout the forebrain and midbrain of the male Syrian hamster. The circles represent enkephalin immunoreactive cell bodies, the squiggly lines represent enkephalin immunoreactive fibers, and the dots represent enkephalin immunoreactive terminal fields. The mapping illustrated here represents a composite of the most consistently labeled regions from six colchicine-treated brains and two non-colchicine-treated brains.

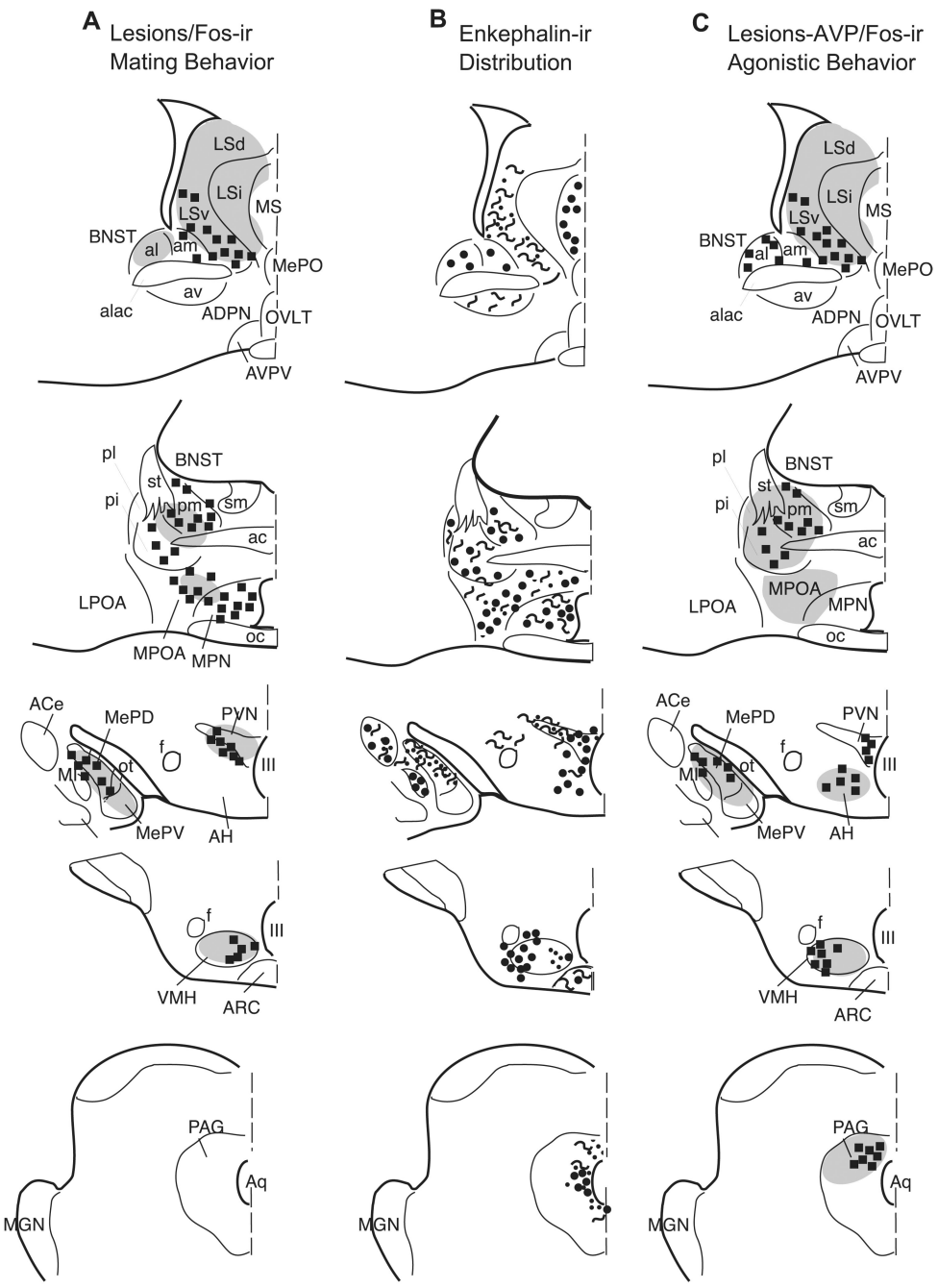

Fig. 15.

Schematic representation of nuclei within the hamster brain where lesions or AVP injections (gray shading) cause a change in either mating (A) or agonistic (C) behavior with an overlay showing Fos production (squares) induced by these behaviors. The enkephalin immunoreactivity reported here is shown in B, where circles=cell bodies, squiggly lines=enkephalin immunoreactive fibers, and dots=enkephalin immunoreactive terminal field.

Table 1

Met- and leu-enkephalin distribution

Region	Methionine enkephalin	Leucine enkephalin
Olfactory system		
Glomeruli of olfactory bulb	cf	–
Anterior olfactory nucleus	cf	cf
Bed nucleus of the stria terminalis	cf	cf
Paleocortex	cf	cf
Hippocampal formation		
Dentate gyrus	cf	cf
CA1	cf	cf
CA3	cf	cf
Anterior continuation of hippocampus	f	−f
Septal region		
Dorsal lateral septum	–	–
Ventral lateral septum	f	f
Intermediolateral septum	–	–
Medial septum	c	c
Diagonal band of Broca	cf	cf
Hypothalamus		
Magnocellular nuclei (SON, PVN)	cf	cf
Medial preoptic area	cf	cf
Ventromedial nucleus	cf	cf
Suprachiasmatic nucleus	cf	cf
Anterior hypothalamus	cf	cf
Lateral hypothalamus	cf	cf
Arcuate nucleus	cf	cf
Amygdala		
Central nucleus of the amygdala	cf	cf
Medial nucleus of the amygdala	f	f
Anterior cortical nucleus of the amygdala	c	c
Posterior basolateral nucleus of the amygdala	–	–
Basal ganglia		
Olfactory tubercle	f	cf
Accumbens, caudate/putamen	cf	cf
Globus pallidus	f	f
Ventral pallidum	f	f
Substantia nigra, pars compacta		
Thalamus		
Anterior nucleus	f	f
Brainstem		
Inferior colliculus	cf	cf

Region	Methionine enkephalin	Leucine enkephalin
Periaqueductal gray	cf	cf
Nucleus locus coeruleus	f	f
Trigeminal sensory nuclei (all)	cf	cf
Raphe nuclei (some)	cf	cf
Nucleus paragigantocellularis	cf	cf
Lateral reticular nucleus	cf	cf
Nucleus tractus solitarius	cf	cf
Spinal cord, dorsal horn	cf	cf

c=cells; f=fibers; –=no immunoreactivity.

Table 2

Mean number of leu-enkephalin immunoreactive cells following incubation with peptide

Brain region	Leu-enkephalin antisera only	Met-enkephalin peptide and Leu-enkephalin antisera	*p*-value
PAG	38.83 ± 2.26	37.17 ± 2.12	0.645
Septum	12.58 ± 2.15	10.08 ± 2.58	0.191

The mean number of leu-enkephalin immunoreactive neurons is not statistically different when comparing tissues incubated with leu-enkephalin antisera only or leu-enkephalin antisera preabsorbed with 75 μM of met-enkephalin in brains injected with 200 μg of colchicine. The table shows the mean number of enkephalin immunoreactive cells±S.E.M. as well as the *p*-value (Student's *t*-test) for each brain region.